Materials Today Bio 16 (2022) 100413

Contents lists available at ScienceDirect

Materials Today Bio

journal homepage: www.journals.elsevier.com/materials-today-bio

Current material engineering strategies to prevent catheter encrustation in urinary tracts

Qin Yao [a], Chengshuai Wu [a], Xiaoyu Yu [a], Xu Chen [b], Guoqing Pan [b], Binghai Chen [a,*]

[a] Department of Urology, Affiliated Hospital of Jiangsu University, 438 Jiefang Road, Zhenjiang, Jiangsu, 212001, PR China
[b] Institute for Advanced Materials, School of Materials Science and Engineering, Jiangsu University, 304 Xuefu Road, Zhenjiang, Jiangsu, 212013, PR China

ARTICLE INFO

Keywords:
Anti-Encrustation
Antibacterial
Ureteric stent
Catheter
Anti-infective coating

ABSTRACT

Catheters and ureteric stents have played a vital role in relieving urinary obstruction in many urological conditions. With the increasing use of urinary catheters/stents, catheter/stent-related complications such as infection and encrustation are also increasing because of their design defects. Long-term use of antibiotics and frequent replacement of catheters not only increase the economic burden on patients but also bring the pain of catheter replacement. This is unfavorable for patients with long indwelling catheters or stents but inconvenient to replace. In recent years, some promising technologies and mechanisms have been used to prevent infection and encrustation, mainly drug loading coatings, functional coatings, biodegradable polymers and metallic materials for urinary devices. Obvious effects in anti-encrustation and anti-infection experiments of the above strategies in vivo or in vitro have been conducted, which is very helpful for further clinical trials. This review mainly introduces catheter/stent technology and mechanisms in the past ten years to address the potential impact of anti-encrustation coating of catheter/stent materials for the prevention of encrustation and to analyze the progress made in this field.

1. Introduction

Urological devices such as catheters and stents are commonly utilized by urologists to treat obstructions through temporary or permanent drainage. The most commonly used catheter today is the Foley catheter, which was introduced by Dr Frederick B Foley in the mid-1930s and is used in hospitals and the community [1]. In 1949, Herdman first described ureteric stents [2]. Thomas Hepperlen and Roy Finney proposed single-J and double-J ureteral stents in the 1970s, which have been in use ever since [2]. The current usage amount is huge and increasing year by year. The indwelling devices mentioned above often lead to complications mainly about pain, discomfort, urinary tract infection (UTI) and encrustation [3,4]. These complications are not only associated with increasing health care costs but also lead to local or systemic symptoms, sepsis, renal failure, and even death [4,5].

Biofilm, made up of bacteria, reducing the antibiotic sensitivity, make UTI easily to occur and difficult to treat [6,7]. Gram-positive bacteria such as *Staphylococcus aureus* (*S. aureus*) and Gram-negative bacteria include *Escherichia coli* (*E. coli*), *Proteus mirabilis* (*P. mirabilis*), *Klebsiella pneumoniae* (*K. pneumoniae*), and *Pseudomonas aeruginosa* (*P. aeruginosa*), which are the most prevalent bacteria. Candida species also grow and reproduce well in the urinary tract microenvironment [8]. Biofilms can also lead to catheter and stent encrustation, especially infections by *P. mirabilis*, *K. pneumoniae*, and *P. aeruginosa*, which can generate urease [9]. Once urea decomposes into ammonia by urease, the pH in urine increases, which causes cations such as Ca^{2+} and Mg^{2+} to deposit on the biofilm to form crystals [10](Scheme 1). Crystals were deposited inside the lumen, which would reduce adequate urine flow and even completely block the lumen, leading to impaired renal function. Moreover, it would deposit on the stent/catheter surface, making stent/catheter difficult to be removed. The suggestions for preventing UTI and encrustation include shorting catheter/stent use, sterile operation, and drinking plenty of water and antibiotics [11–13]. However, these could be cumbersome, ineffective, and short acting.

In this review, an overview of anti-encrustation and anti-infection strategies was presented by focusing on drug loading coatings, functional coatings, biodegradable urinary devices and metallic materials for urinary devices. Current studies on this topic are mainly based on antimicrobial drug loading on urinary devices [14]. Based on the development of biomaterials and catheter preparation technology, strategies of functional coating on urinary devices, biodegradable urinary devices and metallic materials for urinary devices have attracted increasing attention,

* Corresponding author.
E-mail address: chenbhny@ujs.edu.cn (B. Chen).

https://doi.org/10.1016/j.mtbio.2022.100413
Received 19 July 2022; Received in revised form 25 August 2022; Accepted 26 August 2022
Available online 7 September 2022

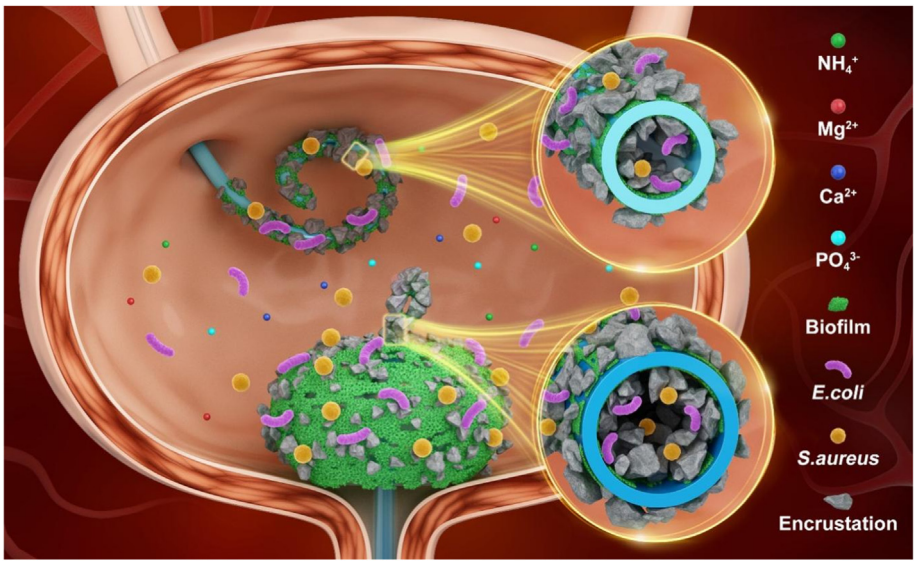

Scheme 1. Schematic of catheter/stent-related infection and encrustation.

which are exactly what we need to focus on after introducing drug loading on urinary devices. Finally, we provide a forecast on this subject based on existing issues and future developments in biofunctionalized applications. We expect this review to not only offer researchers with a clear background of catheter/stent-related complications and research status but also inspire the development of new strategies for inhibiting the occurrence of encrustation and infection and to reduce the pain of patients and the economic burden on families and society.

1.1. Drug loading on urinary devices

1.1.1. Antibiotic drug coating

Antibiotics are effective against bacteria that cause urinary tract infections, and long-term oral or intravenous antibiotics can lead to bacterial drug resistance. Local rather than the systemic of drug use can avoid a certain degree of the development of drug resistance [15]. Triclosan has been widely used for several decades. It can target the enoyl-acyl carrier protein reductase (EACPR), which is a highly conserved enzyme for membrane maintenance involved in fatty acid synthesis in bacteria [16]. Therefore, triclosan can kill bacteria protected by biofilms. Some studies also found that triclosan can decrease the expression and activity of various inflammatory factors [17,18]. Not only is there no evidence that over decades of extensive use of triclosan can develop antibiotic-resistant organisms, but there is also proof that triclosan can reduce the usage of antibiotics and decrease bacterial drug resistance [19–21]. Tian and his colleagues patented a synthesis method of nontoxic waterborne biodegradable polyurethanes (WBPU) [22]. They produced triclosan-loaded WBPU and tested the bacteria by loading WBPU with different concentrations of triclosan in vitro [23]. The results show that it can inhibit *Proteus mirabilis*. *Proteus mirabilis* can form biofilms and increase urinary pH, leading to crystal deposits on the catheter. In an in vitro bladder model, triclosan-loaded WBPU prolonged catheter blockage time and slowed biofilm formation. In this research, no studies have been carried out on other bacteria that cause biofilms and calculi, although there is no evidence that triclosan produces bacterial resistance. Thus, we should also be aware of its resistance.

Belfield and his colleagues produced an antimicrobial urinary catheter (AUC) impregnated with rifampicin, triclosan, and sparfloxacin [24] (Fig. 1A). The appearance of the AUC segments without soaking in artificial urine (AU) was different from that of silicone catheters over a total of 2 weeks (Fig. 1B). In the static model of encrustation with *P. mirabilis*, obviously less phosphate was observed on the surface of the AUC segments compared to the control catheter segments at 48, 72 and 96 h (Fig. 1C). This suggests that AUC can reduce encrustation produced by *P. mirabilis*. In the 26-day flow model, SEM showed fewer crystal deposits on AUC lumens compared to the control group when inoculated with *P. mirabilis* (Fig. 1D). They use multiple antimicrobials of different classes to prevent drug resistance, since the bacteria are very unlikely to be resistant to two or more antibiotics at the same time. In the 28-day test period, compared with the control group, none of the AUCs were blocked. As showed in Fig. 1E, during the 12 consecutive weeks of antibacterial experiment, the bacterial (methicillin-resistant *Staphylococcus aureus* and *E. coli*) colony of AUC group was significantly lower than control group. Which indicated that coating also prevented methicillin-resistant *Staphylococcus aureus*, methicillin-resistant Staphylococcus epidermidis, carbapenemase-producing *E. coli*, and extended-spectrum beta-lactamase-producing *E. coli* adhesion in 12 consecutive weeks (Fig. 1E). All impregnated antimicrobials have been widely used in the clinic for decades, and their safety has been confirmed. What inspires us is the data from a clinical trial of tolerability and acceptability, which shows safety and no evidence of inflammation and toxicity in 30 patients with AUCs [25].

1.2. Silver ion incorporation

Silver is an effective antimicrobial agent approved by the Food and Drug Administration (FDA) to prevent UTI. Because of its oligodynamic activity, silver can destroy bacterial membranes, cause cell protein denaturation, and inhibit bacterial and fungal reproduction [26]. The form of silver polymer coating is mainly about silver alloy (with palladium or gold), silver-containing polymers, and silver nanoparticles (AgNPs). However, the great mass of silver-coated catheters showed ineffective anti-infection and encrustation effects. The reason may lie in the low capability of silver release and the formation of biofilms, which further limits silver release [27,28].

Polytetrafluoroethylene (PTFE) has excellent nonstick ability and reduces the silver release limitation caused by biofilms [29]. A new coating has been developed based on this property: silver-PTFE nanocomposite coating [30]. In the in vitro bladder model (Fig. 2A), the Ag-PTFE-coated catheter significantly prolonged the time of bacteriuria from an average of 6 days (control) up to 41 days ($P < 0.005$) (Fig. 2B). A significantly longer duration of anti-encrustation was found in coated catheters with initial concentrations of 10^6 and 10^3 cells/mL in the bladder [31] (Fig. 2C). Images and SEM showed that the eye hole and the lumen of uncoated catheters were heavily blocked, and little encrustation was visible on the silver-PTFE nanocomposite-coated catheter (Fig. 2D).

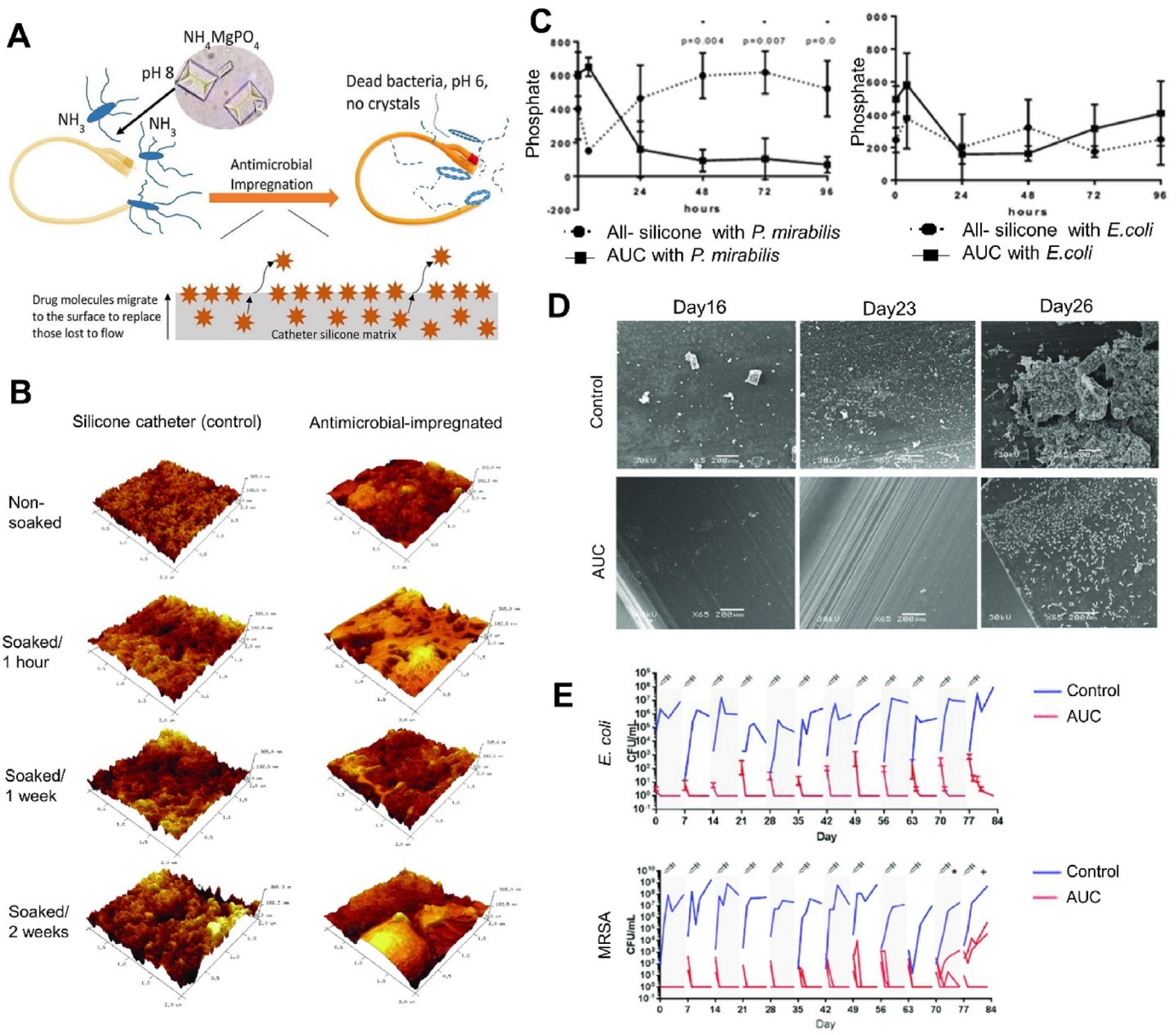

Fig. 1. (A) Scheme of the setup of the in vitro flow model. (B) Atomic force microscopy (AFM 3D height sensor) results of silicone and antimicrobial-impregnated urinary catheters (AUCs) soaked in artificial urine (AU) for 1 h, 1 week, or 2 weeks. (C) Phosphate (mg/L) attached to silicone and antimicrobial-impregnated catheter (AUC) segments incubated statically with *P. mirabilis* and *E. coli* in artificial urine. (D) Scanning electron microscopy (SEM) images of the lumens of silicone (control) and antimicrobial-impregnated urinary catheters (AUCs) perfused with artificial urine and inoculated with *P. mirabilis*. (E) Examples of colonization of silicone controls and antimicrobial urinary catheters (AUCs) by NDM-1-producing *E. coli* and MRSA. Reproduced with permission from ref 24, Copyright 2019, Elsevier BV.

The MTT assay showed no significant cytotoxicity compared to silicone catheters ($P < 0.1$). In the cytotoxicity assay, there were no dramatic differences in cell growth among the blank wells, wells with uncoated catheter segments and wells with coated catheter segments (Fig. 2E). The MTT assays showed that, comparable to the control silicone samples, cell viability in silver-PTFE nanocomposite-coated catheter segments were higher than 90% ($P > 0.1$) (Fig. 2F). It has the advantage of anti-encrustation properties, but further animal studies should be performed to verify its further performance.

PDPA, which is a surface anchor, can be coated onto almost any material surface, including silicone [32]. Poly(sulfobetaine methacrylate-*co*-acrylamide)[poly(SBMA-*co*-AAm)] can inhibit the formation of biofilms and adhesion of bacteria [33]. selected as the final layer of the coating. AgNP-PDPA, bilayers with grafted poly (SBMA-*co*-AAm) (P3) as an anti-biofilm and anti-encrustation coating, was successfully developed by Wang and his colleagues [28]. This coating can effectively reduce bacterial adhesion and biofilm formation. In the in vitro model, compared with the Dover™ silver-coated catheter (time of resistant encrustation 7 days), the P3-coated catheter can resist crystal deposits for 45 days. In a mouse model, *E. coli* biofilm was detected on only one out of four P3-coated catheters; however, biofilm formation was shown in five out of six uncoated catheters. Compared to the Dover™ catheter, the deposition of calcium and magnesium in the bladder of pigs with a P3-coated catheter was reduced by 1.8 times. No cytotoxicity was observed in pigs or mice [34].

Hydrophilic poly (*p*-xylylene) PPX-N, a biocompatible polymer, increases the silver ion release rate and improves the wettability of the catheter. Thus, the silver/hydrophilic PPX-N coating can inhibit bacterial adhesion, prevent the biofilm formation of *E. coli* and *S. cohnii*, and reduce encrustation compared with the bacteria-only control in vitro

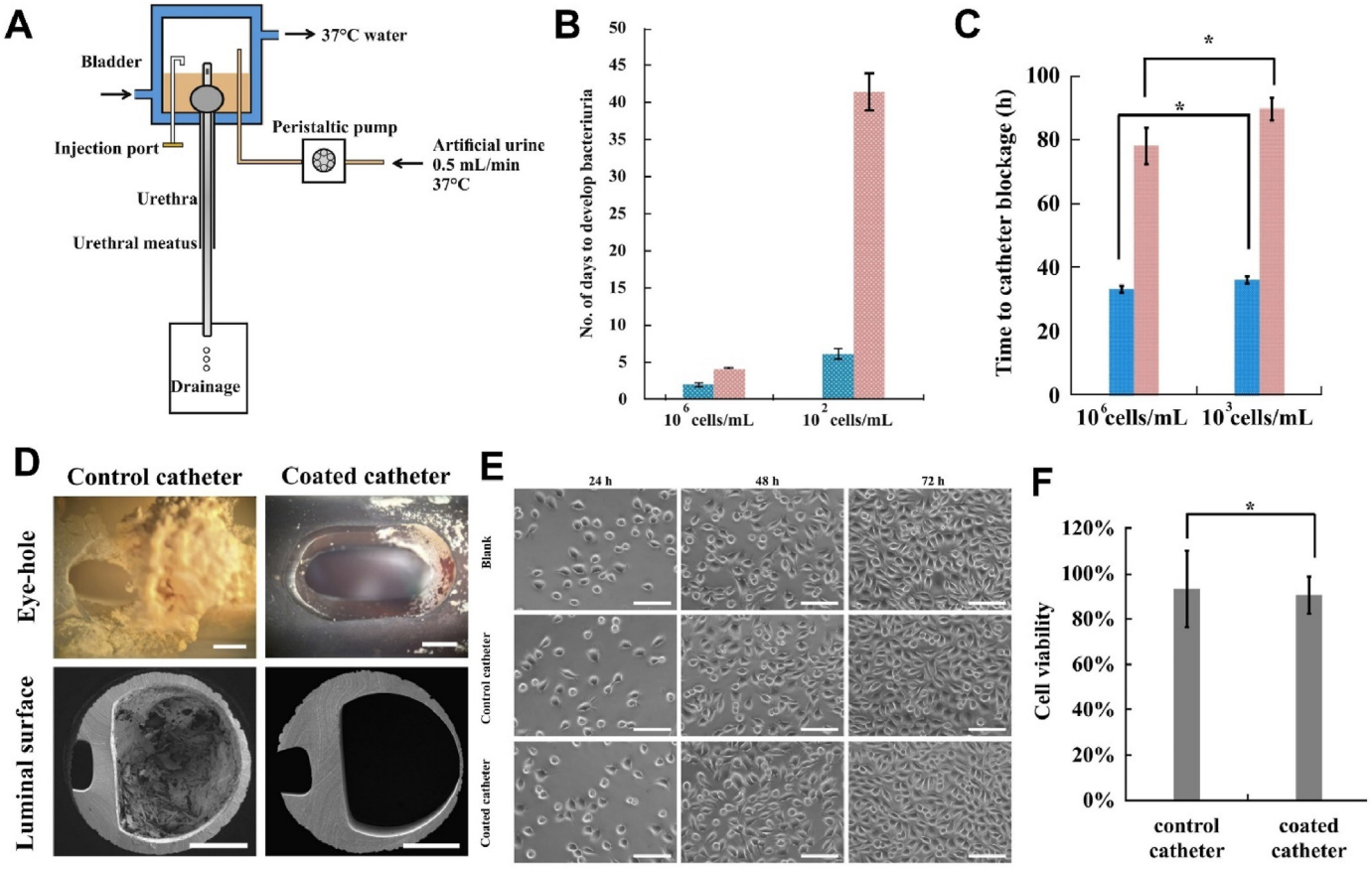

Fig. 2. (A) Schematic diagram illustrating in vitro bladder models to study. (B) Time taken to develop bacteriuria in the bladder model for evaluation of the antibacterial performances of whole silicone (control) and Ag-PTFE nanocomposite-coated catheters. (C) The time to blockage of silicone (control, blue bar) and Ag-PTFE nanocomposite-coated (red bar) catheters in the bladder model. (D) Optical images of eye-hole sections and scanning electron microscope images of lumen sections. Scale bar: 1 mm. (E) Growth curves and optical images of cells on well plates under direct incubation with catheter segments. Scale bar: 100 mm. (F) MTT assays of extracts from catheter segments. Reproduced with permission from ref 31, Copyright 2017, Elsevier. (For interpretation of the references to colour/colour in this figure legend, the reader is referred to the Web version of this article.)

model [35]. Although it showed excellent resistance to biofilm and crystal deposits, its cytotoxicity and effectiveness in an in vivo model need further investigation.

1.3. Silver and antibiotic hybrid coating

Silver combined antibiotics can offer a synergistic antibiotic effect, and the coating combined silver and antibiotics not only improve the ability of antibiotic effect but also help address antibiotic resistance [36,37]. Norfloxacin, a fluoroquinolone with a hydrophobic nature that has broad-spectrum antimicrobial properties, is used to treat UTI caused by gram-positive and gram-negative bacteria [38,39]. This kind of antibiotic can inhibit the DNA-gyrase enzyme, which is essential in bacterial DNA synthesis [40]. The ionized form of silver is also a broad-spectrum antibacterial agent. It rarely develops into bacterial resistance since it can attack broad sites within the bacterial cell [41]. To avoid silver nanoparticle aggregation, they were coated with tetraether lipids (TEL). TEL-coated silver nanoparticles were distributed in a hydrophobic film of poly (lactic-*co*-glycolic acid) (PLGA) loaded with norfloxacin [42]. This kind of coating is called tetraetherlipid-Ag-norfloxacin-polylactid (TANP) (Fig. 3A). The burst release of norfloxacin from the PLGA film was observed in the first few days. The burst release rate in the first few days was approximately 60%, and the slow-release rate in the next 50 days was approximately 40% (Fig. 3B). In vitro bacterial and encrustation tests showed that, compared with the uncoated catheter, the coating could inhibit the adhesion of bacteria effectively and decrease the viability of bacteria (Fig. 3C). It can also efficiently reduce the encrustation on the surface (Fig. 3D and E). Of note, they established an in vitro encrustation model to evaluate the multifunctional biomaterial effect on biofilm formation and crystallization. They grafted the coating onto a silicone (SIK) catheter and polyurethane (PUR) ureteral stent and used this model to carry out in vitro crusting experiments over 14 days. The concentration of dead bacteria observed on the TANP-coated surfaces was much higher than that on the control surface (Fig. 3F). On average, the concentration increased from ~12% to ~41% for PUR and from ~27% to ~67% for SIK samples. The volume of biofilm is reduced by 75% [43]. The study shows that the time of norfloxacin release from PLGA is up to 52 days, which is very beneficial for patients with long-term indwelling catheters.

Silver sulfadiazine is a broad-spectrum bactericidal antimicrobial that can effectively treat gram-positive and gram-negative bacteria by destroying DNA replication, directly modifying the lipid cell membrane, and forming free radicals [44,45]. This antibiotic was previously used to treat burns and can inhibit bacterial colonization. In 2017, a clinical trial comparing silver sulfadiazine-coated ureteral stents with bare stents for 4 weeks showed that silver sulfadiazine-coated stents decreased bacterial colonization more than control stents on the stent surface, and the difference in stent culture between the control group and antibacterial group was statistically significant ($p = 0.054$) [46]. Due to the short duration of stenting and the relatively small sample size, it is impossible to prove its effect on biofilm formation, encrustation or infection development in patients with long-term stents [46]. The silver and antibiotic

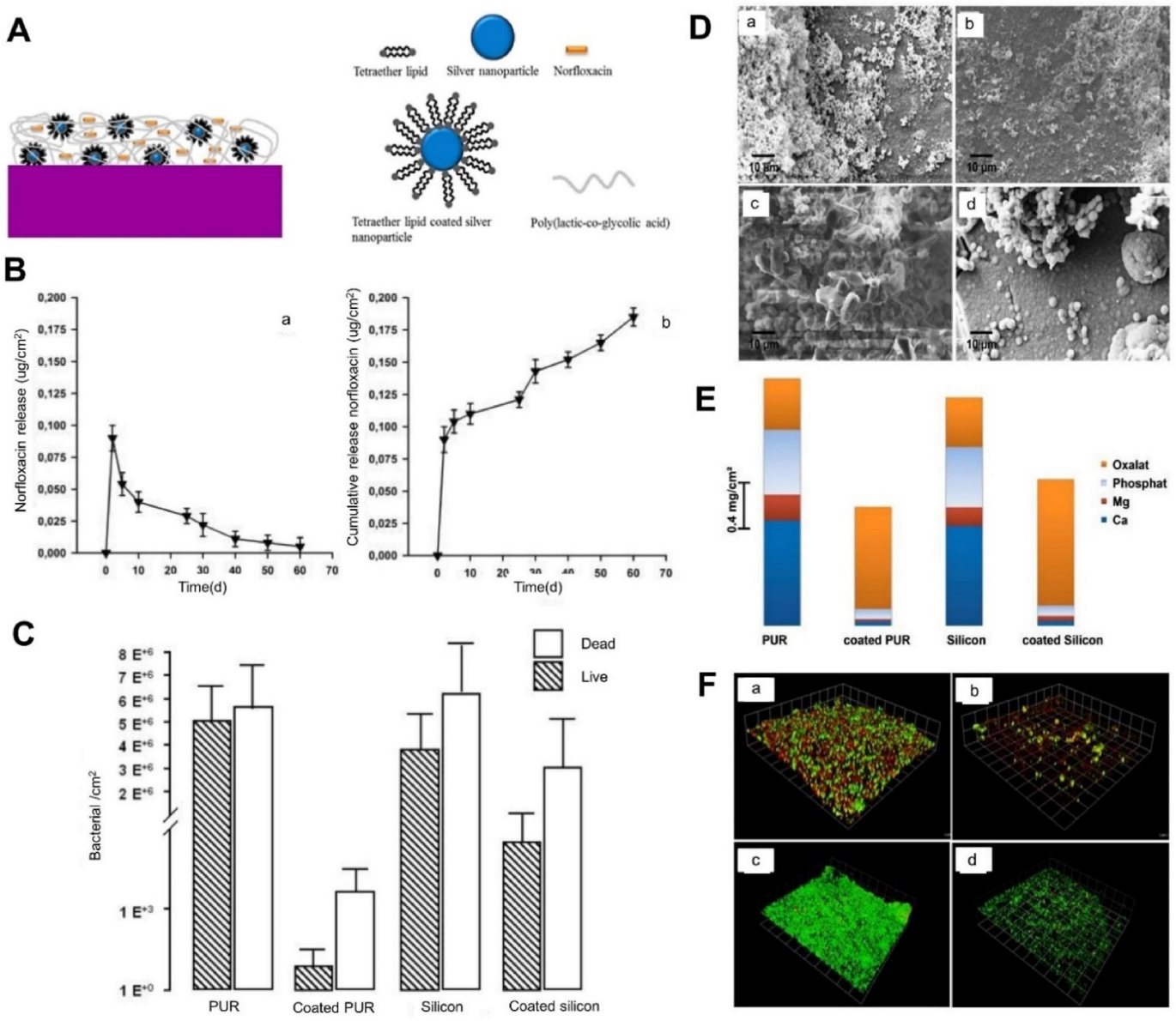

Fig. 3. (A) Schematic representation of PLGA//TEL-Ag/NF construction. (B) Sustained (a) and cumulative (b) release profiles of norfloxacin in PBS at 37 °C. (C) Measurement of bacterial adhesion and viability on unmodified and modified PUR and silicon sheets. (D) Scanning electron microscopic images, 1000x on unmodified PUR and silicon (a and c, respectively) and film-coated PUR and silicon (b and d, respectively). (E) Mass of Ca, Mg, phosphate and oxalate in the crystalline deposits formed on both modified and unmodified PUR and silicon sheets. (F) CLSM imaging of adhered live and dead bacteria on unmodified PUR and silicon (a and c, respectively) and film-coated PUR and silicon (b and d, respectively). Reproduced with permission from ref 42, Copyright 2017, Elsevier. (For interpretation of the references to colour/colour in this figure legend, the reader is referred to the Web version of this article.)

mixed coating has been proven to have the effect of antibacterial adhesion both in vitro and in vivo. Our purpose is not only to study its anti-adhesion effect but also to study its anti-encrustation ability. There is no related research in the above clinical trials, which may be a focus that we need to study in the future.

1.4. Antibacterial peptide coating

Antimicrobial peptides (AMPs) are a set of natural host defense peptides [47] that have been revealed to have various functions, including controlling immune responses, stimulating the accumulation of immune cells at the site of infection, anti-inflammatory and neutralizing endotoxin properties, stimulating angiogenesis and accelerating wound repair. Due to their unique structure of cationic and amphipathic residues, AMPs can target the lipopolysaccharide layer of the cell membrane to disrupt the cell wall and then kill bacteria [48–53]. In addition, AMPs have the abilities to increase the susceptibility to the antimicrobial drug by entering into the bacteria and interact with the lipid bilayer to form a transmembrane pore and to inhibit the formation of biofilms that are resistant to most antibiotics [54–56]. Other killing bacterial mechanisms of AMPs include inhibiting intracellular functions, extracellular polymeric organisms, intracellular translocation, and the synthesis of DNA/RNA/protein [55,57]. As one of the most promising alternatives to antibiotics, AMPs have shown promise to improve the outcome of medical devices with a high risk of infections.

Covalent immobilization of AMPs on a surface as an antimicrobial coating has been used as a strategy to prevent the need for further and extra systemic treatment [58–61]. One covalent immobilization strategy for surface modification was a bioinspired chemistry based on the oxidative self-polymerization of dopamine (DPA) developed by Lee et al.

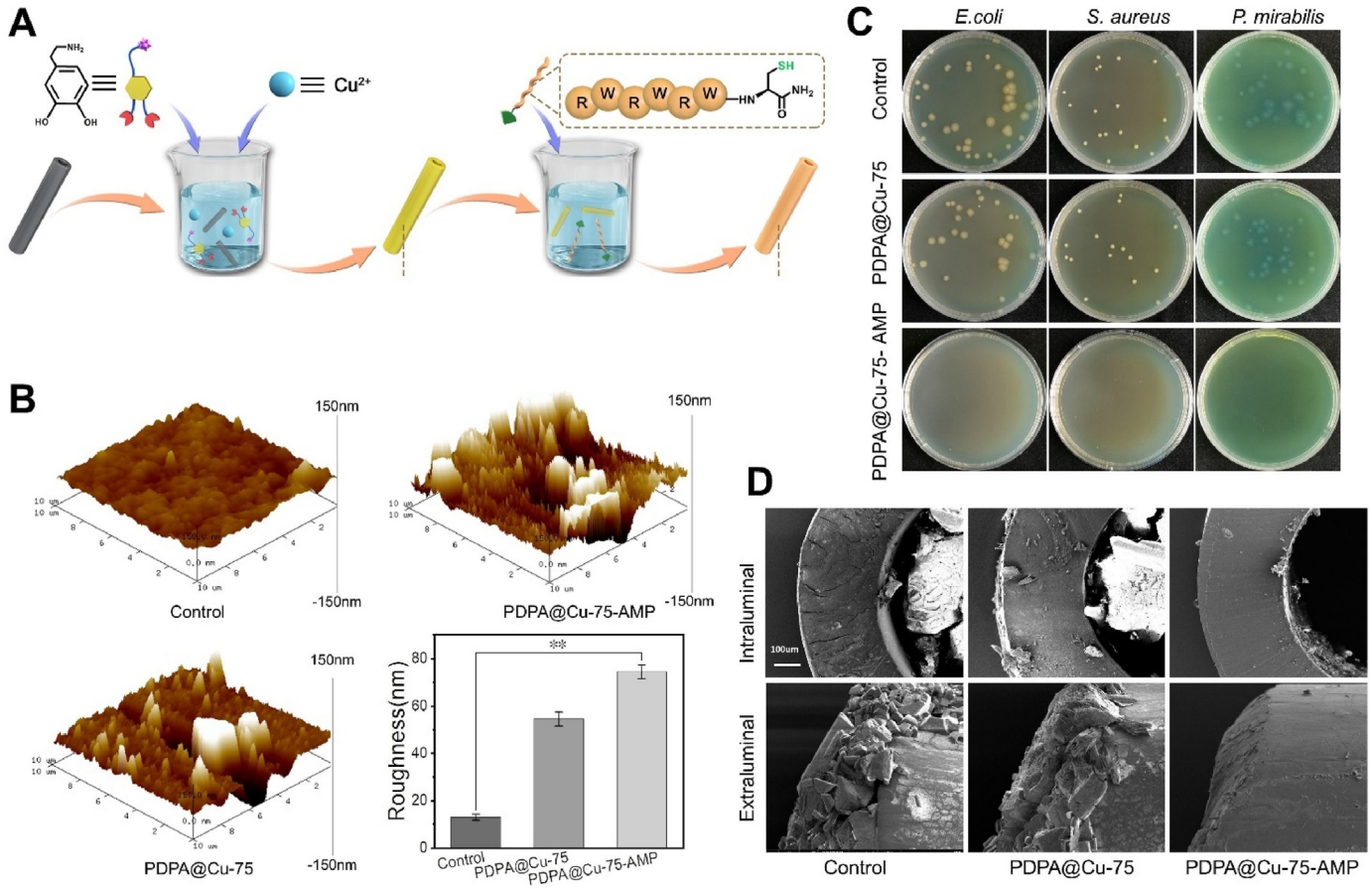

Fig. 4. (A) The molecular structures of DOPA and AMPs and the synthesis process of the bioinspired antibacterial coating. (B) AFM and roughness of the bare PU sheet, PDPA@Cu-75 coating and PDPA@Cu-75-AMP coating on PU sheets. Statistically significant differences are indicated by *p < 0.05 or **p < 0.005 compared with the control group. (C) Antibacterial effect of bare stents (control), PDPA@Cu-75 and PDPA@Cu-75-AMP coating against *E. coli*, *S. aureus* and *P. mirabilis*. (D) SEM of rat intravesical stent lumens and deposit surfaces in the control, PDPA@Cu-75 and PDPA@Cu-75-AMP coating groups. Reproduced with permission from ref 76, Copyright 2021, Royal Society of Chemistry.

in 2007 [62]. This was inspired by the coexistence of catechol and amine in mussel foot proteins and by synergistic salt displacement of catechol and amine at the solid–liquid interface to form a synergistic interface adhesion [63–66]. Through catechol-metal coordination, π-π interactions, electrostatic interactions, covalent reactions and hydrogen bonding, the deposition of polydopamine (PDPA) can occur on almost all types of materials [67–69]. This mussel-inspired chemistry has the property of allowing functionalization of biomolecules on a variety of biomaterials through amino- or thiol-mediated Michael addition [70–73]. Metal-catechol-assisted mussel chemistry was used for a typical AMP (RWRWRWC-NH_2) with thiol group functionalization on commercially available stents (Fig. 4A) [74–76]. Both AFM characterization and roughness compared with uncoated stents showed that the coating was successfully grafted onto the surface of stents (Fig. 4B). In this work, Yao et al. evaluated its bactericidal and anti-crusting ability both in vitro and in vivo [76]. In the in vitro antibacterial experiment, the stents with AMP coating inhibited *E. coli*, *S. aureus* and *P. mirabilis* growth and biofilm formation in situ (Fig. 4C); even after 2 weeks, the coating also showed good antibacterial effects. In addition, the coating not only had good biocompatibility but also reduced the deposition of struvite and hydroxyapatite crystals in 2 weeks of in vivo experiments (Fig. 4D) [76]. This study developed a safe, stable, and effective antibacterial coating on urinary tract medical devices for long-term bacterial inhibition and encrustation prevention.

Another covalent immobilization strategy was (1-mercapto-11-undecyl)-(tetra(ethylene glycol) (EG4), 1,1′-carbonyldiimidazole (CDI), and self-assembled monolayers (SAMs) immobilized Chain201D AMP (AMP-CDI-EG4-SAMs) (Fig. 5A) [48]. In an in vitro antibacterial experiment, the AMP-CDI-EG4-SAM coating was highly effective against strains relevant to urinary catheter-associated infections (including clinical bacterial strains such as *E. coli*, *K. pneumoniae*, *Enterobacter cloacae* (*E. cloacae*), *P. aeruginosa*, *A. baumannii* and *S. aureus* and clinical strains of yeasts such as *Candida albicans* (*C. albicans*), *Candida glabrata* (*C. glabrata*) *and Candida parapsilosis* (*C. parapsilosis*)) and was stable over a wide range of temperatures (up to 45 °C), pH values (4–9) and salt concentrations (50, 100 and 200 mM NaCl) [48]. This antibacterial property has potential anti-crusting ability, and high stability is beneficial to the long-term use of indwelling catheters or stents.

Except for AMP-CDI-EG4-SAMs, the AMP modification strategy on the surface of PU stents attached by novel polymer-based tethering was also an effective surface modification strategy, which not only had non-fouling characteristics but also provided specific flexible binding sites for peptide conjugation (Fig. 5B). In vitro, the use of AMP (E6) conferred excellent antimicrobial activity toward *P. aeruginosa*, *S. aureus* and *S. saprophyticus* while providing strong biocompatibility (Fig. 5C). Importantly, as observed by imaging luminescent-tagged bacteria using the Interactive Video Information System (IVIS), the polymer brush-AMP coating showed a marked reduction in bacterial adhesion in a mouse CAUTI model compared with the control group at 1 and 7 days (Fig. 5D) [77]. This study provides a method of AMP immobilization to prevent and limit the occurrence of CAUTIs.

Three strategies of AMP immobilization as coatings above for medical devices, including ureteric stents or catheters, provide excellent candidates for further development owing to their excellent anti-adhesive,

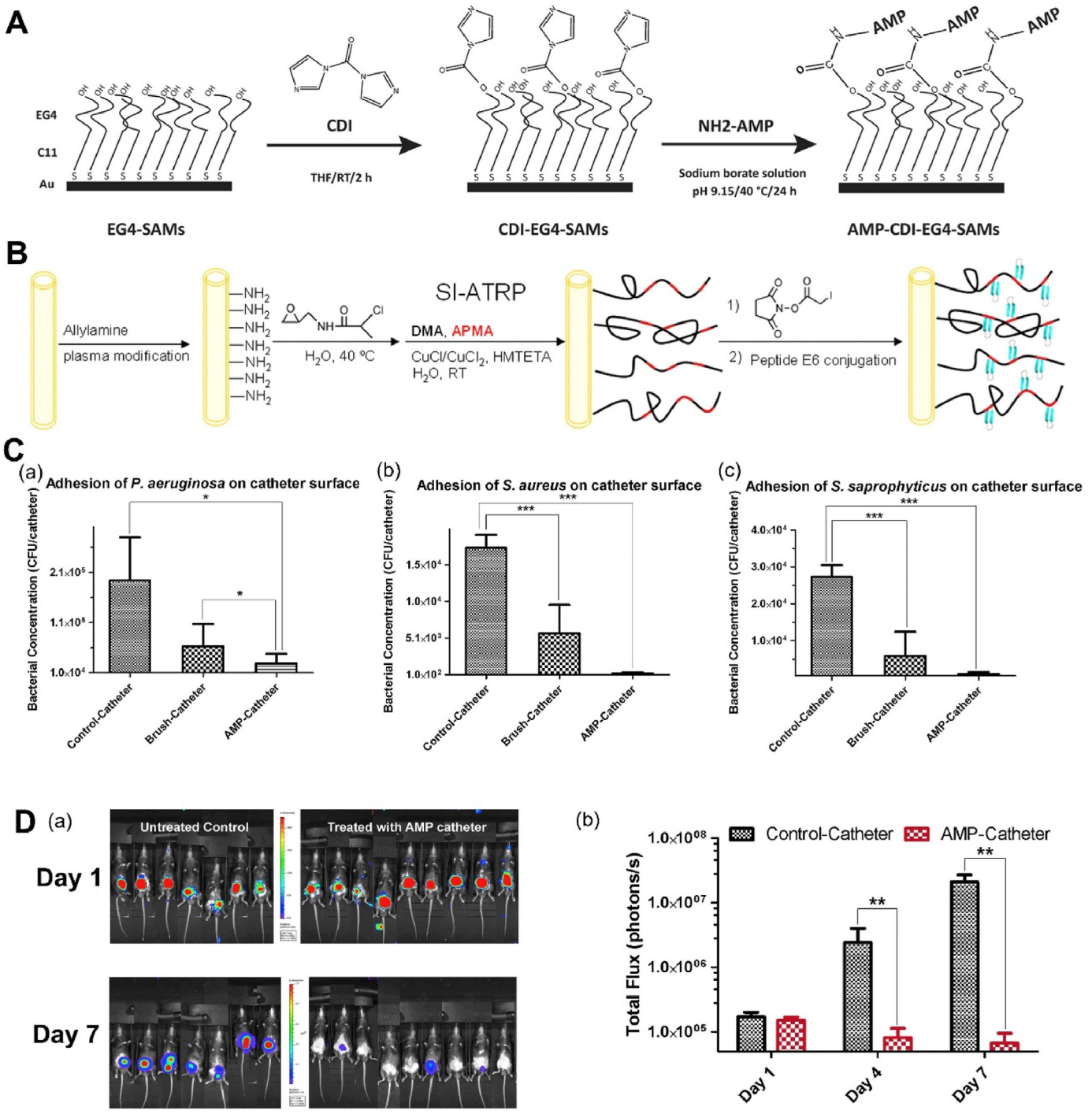

Fig. 5. (A) Schematic representation of AMP (Chain201D) immobilization on EG4-SAMs. (B) Functionalization of polyurethane catheter with AMP-brush coating. (C) Broad spectrum activity of the AMP-conjugated PU catheter against *P. aeruginosa* (a), *S. aureus* (b) and S. saprophyticus (c) in vitro. *Indicates $P \leq 0.05$ and ***indicates $P \leq 0.001$. (D) Antibacterial activity of the AMP-coated PU catheter in a urinary infection model in vivo. (a) IVIS images of mice bearing either untreated or AMP-coated PU catheters at day 1 and day 7 post-instillation with luminescent-tagged *P. aeruginosa* into the bladder. (b) Bioluminescence readings (total photon flux (photons/s)) measured for untreated and AMP coating-treated mice using IVIS Lumina at day 1, 4 and 7 days post-bacterial instillation into the mouse bladder. ** indicates $P < 0.01$. Reproduced with permission from ref 48, Copyright 2019, Nature Publication Group and ref 77 Copyright 2016, Elsevier BV.

antimicrobial and biocompatible properties against bacterial adhesion, colonization and infection. Owing to the natural properties of biofilm formation inhibition and the excellent antibacterial and anti-encrustation properties of coatings, antibacterial peptide coatings are expected to become a potential advantage of anti-encrustation urinary catheters or stents for clinical use, which needs further investigation for verification.

1.5. Drug-loaded polymer modification

Poloxamers, a series of copolymers, contain a central hydrophobic poly segment and two polyethylene oxide (PEO) chains. The central hydrophobic poly segment is used to load and release the fluoroquinolone antibiotic ofloxacin, and PEO chains keep the bacteria away from the surface [78]. Poloxamer 188 molecules were functionalized

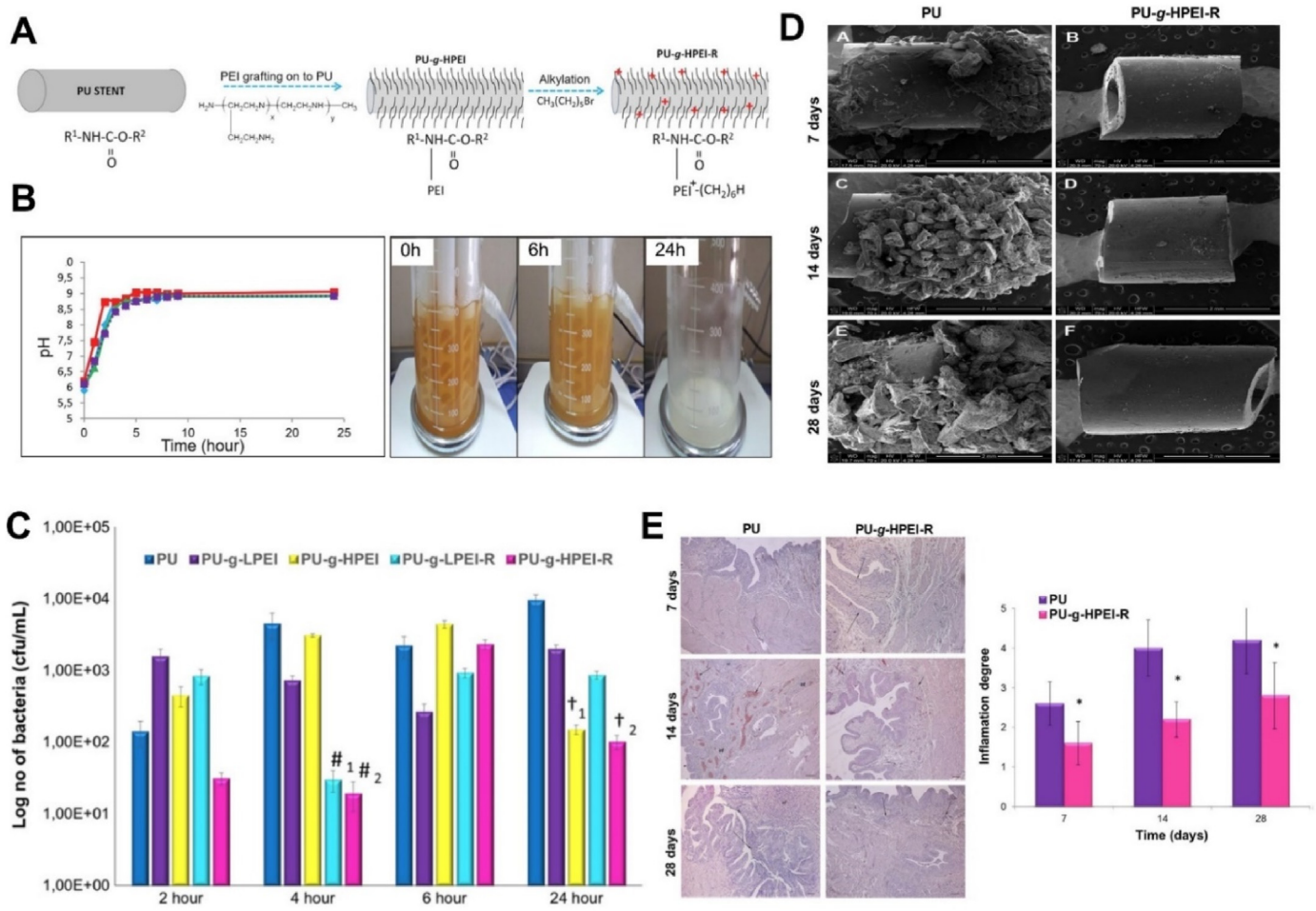

Fig. 6. (A) The reaction steps of PEI brush grafting on the PU stent surface and N-alkylation of PEI brushes. (B) The change in pH during the in vitro encrustation experiment and step-by-step encrustation in the bioreactor system at 0 h, 6 h and 24 h. (C) 2, 4 and 6 h of bacterial adherence and 24 h of biofilm formation test against *P. mirabilis* in biofilm reactor. (D) Encrustation on the ureteral stent samples removed from the rat bladder after 7, 14 and 28 days of implantation. (E) Hematoxylin eosin (H&E) staining micrographs of the rat bladder following urethral stent implantation for different time periods and the histopathological scoring system in terms of inflammation degree in the rat bladder. (Histology score system; 1 = Normal, 2 = Mild inflammation, 3 = Mild–Moderate, 4 = Moderate, 5 = Moderate–Severe, 6 = Severe). * Indicates the significant decrease in PU-g-HPEI-R samples in comparison to PU after 7, 14 and 28 days ($p < 0.05$). Reproduced with permission from ref 92, Copyright 2017, John Wiley and Sons.

with methacryloyl moieties (synthesis of mono- and dimethacrylated poloxamer 188 (MMP and DMP)) and then subsequently copolymerized with hydrogel monomer 2-HEMA (p(MMP/DMP-co-HEMA)) to further promote the function of poloxamer derivatives as cross-linking agents. After testing, when the weight of MMP/DMP is 10% of HEMA, their comprehensive performance is the best. Compared with the control group (contact angle, mean ± S.D.: advancing 91.3 ± 1.65, receding 92.5 ± 1.35), the contact angle shows that 10%p(MMP-co-HEMA) (advancing 98.0 ± 3.75, receding 98.1 ± 4.75) has higher hydrophobicity than 10% p(DMP-co-HEMA) (advancing 92.7 ± 1.25, receding 94.1 ± 1.15. However, 10% p(DMP-co-HEMA) has a higher ultimate tensile strength and Young's elastic modulus. After suspended in artificial urine for a week, the content of calcium ions on the 10% p(MMP-co-HEMA) coating decreased by 87% and magnesium by 92% compared with the poly (hydroxyethyl methacrylate) (p(HEMA)) control. The 10% p(MMP/DMP-co-HEMA) coating reduced the surface adherence of *E. coli* by more than 90% relative to the control p(HEMA) [79]. However, in the drug release experiment, they released earlier and more than the control group, so it was difficult to be of long-term antibacterial.

1.6. Bacteriophage coating

Bacteriophages are natural predatory viruses that replicate inside bacteria. In particular, lytic phages can cause the bacterium to lyse by replicating [26]. Bacteriophages have the advantages of high strain specificity, self-replication and easy genome editing, which can protect normal flora, low-dose treatment of diseases and specific treatment for specific infections [80–83]. The phage was prepared on the surface of the catheter with PVA hydrogel. The bacteriophage release is controlled by the pH-sensitive trigger (self-quenching dye 5 (6)-carboxyfluorescein), which is on the outermost surface of the coating. The pH-sensitive trigger will degrade when the urine pH increases, and the bacteriophage in the lower layer will be released. The in vitro bladder showed that the blockage time of the phage-coated catheter was twice as long as that of the control group ($P = 0.0199$) [84]. It is inferred that bacteriophages can only slow down the time of encrustation but cannot completely prevent it [85]. This phenomenon may be due to a decrease in the amount of bacteriophage released at a later stage. At the same time, although phage cocktail treatment can guard against resistance, the drug resistance of bacteriophages is also a reason for failure to prevent encrustation that cannot be ignored.

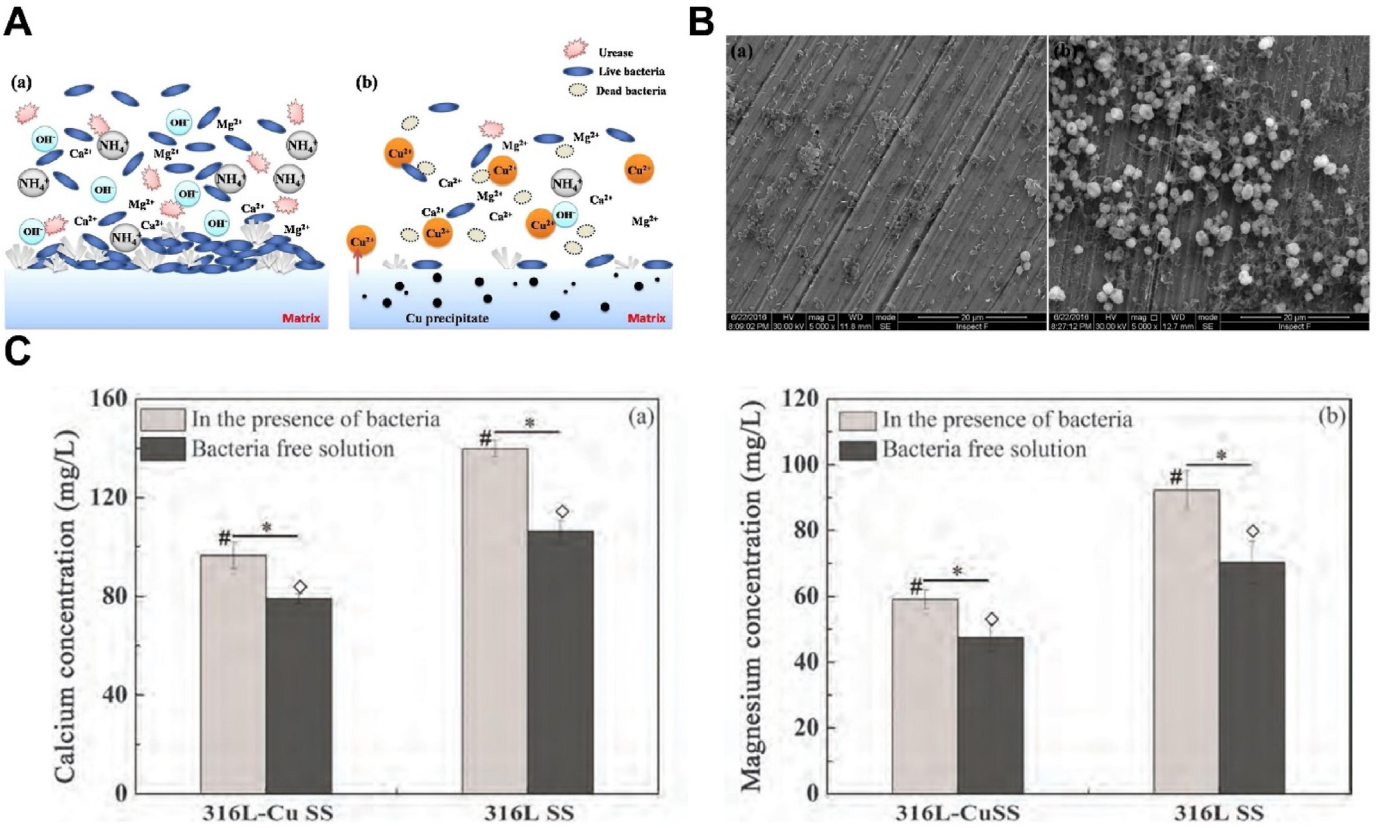

Fig. 7. (A) Mechanism of 316 L-Cu SS inhibiting infectious encrustation: (a) 316 L SS, (b) 316 L-Cu SS. The release of Cu^{2+} ions from 316 L-Cu SS killed the majority of bacteria that produced urease. The hydrolysis of urea was inhibited, resulting in restricting the elevation of Ph. Fewer crystals were deposited on the surface of 316 L-Cu SS. (B) Crystalline deposits on the surface of samples: (a) 316 L-Cu SS, (b) 316 L SS. (C) Ca (a) and Mg (b) contents in the encrustation on different materials by *S. aureus*. Models infected with *S. aureus* (5×10^5 cfu/ml) were supplied with mixed HU and AU solutions. Each value is the mean calculation from three replicated experiments. *, # and ◆ indicate significant differences from the control values at $p < 0.05$. Reproduced with permission from ref 131, Copyright 2017, Elsevier BV.

2. Functional coating on urinary devices

2.1. Polyether-based coating

Pellethane, a kind of aromatic polyether, features flexibility, high strength, and resistance to highly caustic solvents. In the in vitro bladder model, encrustation experiments of pelthane thermoplastic polyurethane (TPU), poly 2-hydroxyethyl methacrylate (HEMA)-coated TPU, tetraethylene glycol dimethyl ether (TETRA)-coated TPU and radio opaque hydrogel-coated ureteral stents (Cook Medical, Inc.) were carried out for 90 days and evaluated for surface crusts. HEMA, a hydrophilic polymer, has the ability to stabilize and resist cell adhesion. Therefore, it is often used as a contact lens material to reduce or prevent the negative effects of biofilms on the surface of the eyes [86]. TETRA is a precursor molecule that may form a hydrophilic linear polymer, whose structure resembles poly (ethylene glycol). TETRA can resist protein adsorption and platelet adhesion under flow conditions [87,88]. The result show that after 90-day trial, all the average mass of magnesium, calcium, and phosphorus were as follows: stent 0.067 mg, 0.312 mg, 1.149 mg, pellethane TPU 0.022 mg 0.164 mg, 0.348 mg, HEMA coated pellethane TPU 0.006 mg, 0.052 mg, 0.360 mg and TETRA-coated pellethane TPU 0.027 mg, 0.183 mg, 0.530 mg. Compared with traditional urinary device material, HEMA-coated pellethane TPU has better anti-encrustation performance [89]. The ant-encrustation effect of HEMA-coated pellethane TPU in vitro experiments for up to 90 days also shows that it is very suitable for patients with long-term indwelling catheters/stents. At present, there are only data from in vitro experiments; more experiments in vivo or clinical trials are needed to obtain more comprehensive data in the future.

Polyethyleneimine (PEI) (Fig. 6A) is a cationic polymer that can inhibit bacterial adhesion [90] and improve antibacterial properties by disrupting the membrane when in contact with bacteria. This antibacterial activity has also been proven to be effective against common urinary bacteria such as Pneumococcus, *E. coli* and *P. mirabilis* [91]. Urea was decomposed by *P. mirabilis,* and the pH increased. The increase in pH promoted encrustation (Fig. 6B). PEIs with different molecular weights (Mn: 1800 and 60,000) are grafted onto the surface of the PU catheter. This positive charge density on the surface of PEI can be made, and the antibacterial property can be further improved when PEI is alkylated. The in vitro model showed that high molecular weight (Mn 60,000) and alkylated PEI could effectively inhibit biofilm formation (Fig. 6C), prevent the deposition of surface crystals, reduce calcium salt and magnesium salt by 81% and 93.4%, respectively, and inhibit bacterial adhesion by 2 orders of magnitude compared with the control group. In the 28-day-old mouse model, there was no obvious crystal deposit on the surface of the high molecular alkylated PEI brush coating (Fig. 6D), and the tissue sections of the mice also showed that its inflammatory response to the host was much weaker than that of the uncoated PU (Fig. 6E) [92]. Polyethyleneimine brushes show excellent performance and a low degree of inflammation, but further clinical trials are required to verify their effectiveness and safety in vivo.

2.2. Polyvinylpyrrolidone-iodine coating

Several studies show that the hydrophilicity of the material surface, such as hydrogel coating, inhibits the catheter surface crust to some extent [93]. Polyvinylpyrrolidone-iodine (PVP–I), a hydrophilic macromolecular material, was used for bladder irrigation to prevent urinary tract infection. This antibacterial material is not an antibiotic and may

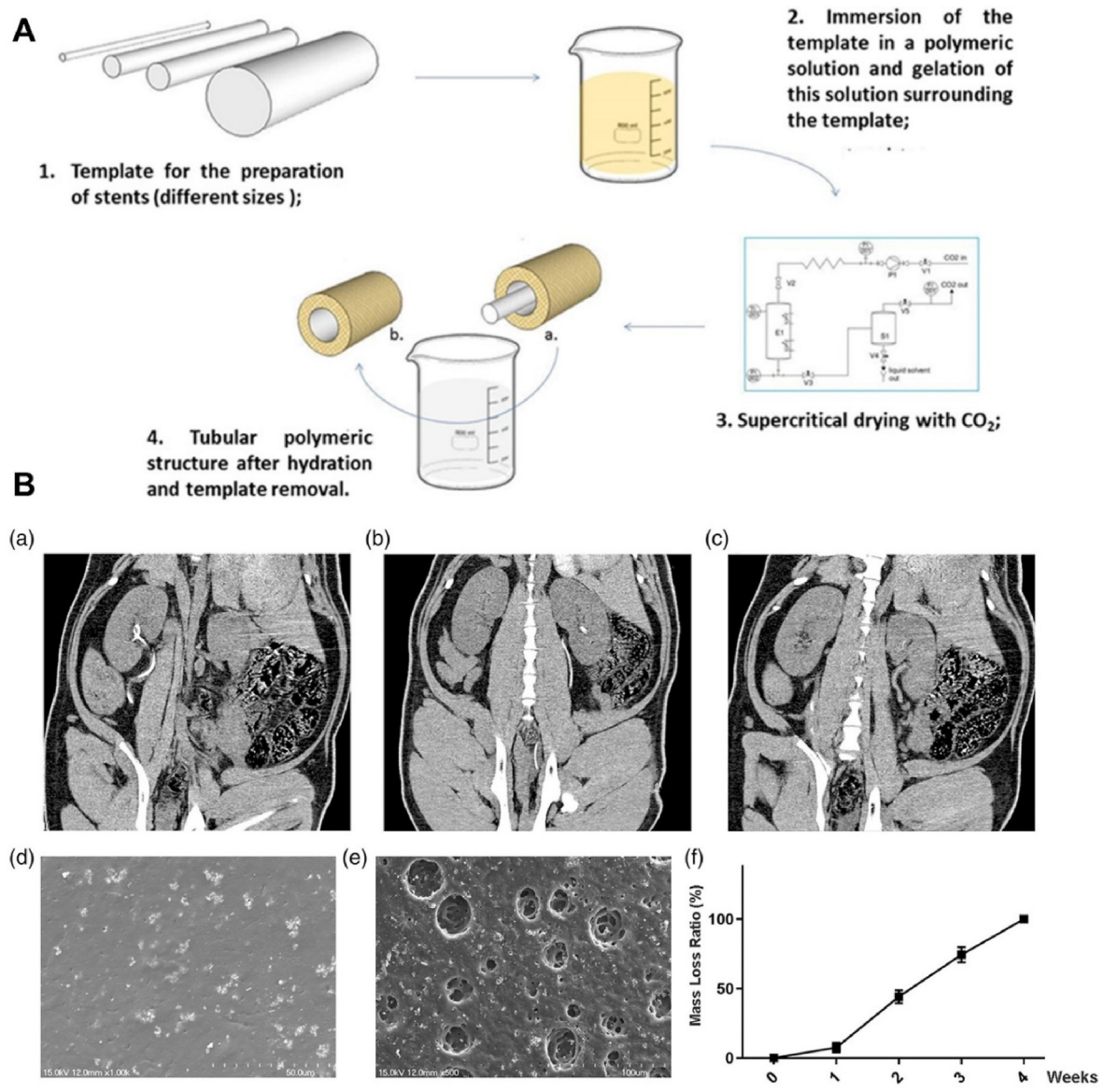

Fig. 8. (A) Methodology used to generate the different stents. (B) Degradation of the stents in vivo. (a). One week after stent implantation, there were no obvious changes. (b). Two weeks after stent implantation, the distal end had degraded. (c). Three weeks after stent implantation, the proximal end remained. (d). SEM image of the stent. (e). SEM image of the stent implanted in the animals for 1 week. (f). Mass loss ratio of the stent in vivo. Reproduced with permission from ref 107, Copyright 2014, John Wiley and Sons and ref 111, Copyright 2020, John Wiley and Sons.

greatly reduce the production of drug-resistant bacteria. PVP-I was embedded on the surface of PU, and AFM showed that the surface of PVP-I was rougher than that of PU and that both sides of the PU/PVP-I film were uniformly covered with PVP-I molecules. The contact angle results showed that the hydrophilicity on the PVP-I coating was significantly improved and that the coating was stable in ultrasonication methods. After a 4-h bacterial adhesion test, the PU/PVP-I surface significantly reduced the adhesion of both *Pseudomonas aeruginosa* ($P < 0.05$) and *Staphylococcus aureus* ($P < 0.01$). SEM images of *P. aeruginosa* and *S. aureus* adhesion also showed that fewer bacteria adhered to the surface of the PU/PVP-I film than to PU. In a 2-week in vitro encrustation model, the surface of the PVP-I coating was only partially covered by crystal deposits, far less than the PU surface [94]. The major encrustation components calcium, magnesium and phosphorous on the PU surface were much higher than those of PU/PVP-I according to energy dispersive X-ray mapping. In summary, PU/PVP-I has good antiadhesion and anti-encrustation properties and has good durability. Until now, few in vivo investigations have been performed. Thus, it is urgent to study its effect on animal models before we can make conclusions.

2.3. Papain immobilized polyurethane

Papain, a food-grade enzyme found in many natural products, was the first cysteine protease isolated from papaya [95,96]. It is covalently cross-linked on polyurethane using glutaraldehyde. This method makes papain more stable and cytocompatible, which means 90% of papain in the solution is immobilized on PU, 88% of which still retains their natural activity. Even after storage at 48 °C for 30 days, the enzyme activity decreased by 15%. In addition, it has better hydrophilicity. MTT showed that when grafted onto PU, the cytocompatibility was significantly higher than that of bare PU ($P < 0.05$). In vitro antibiofilm, bacterial attachment and anti-encrustation experiments indicated that papain-immobilized PU exhibited better antibiofilm ability and less bacterial (*E. coli* and *S. aureus*) attachment than bare PU ($P < 0.01$). In a week of the

Table 1
Material engineering strategies to prevent catheter encrustation.

Category	Anti-encrustation strategies	Anti-encrustation mechanism	References
Drug loading on urinary devices	Antibiotic drug coating	Antibacterial	[22,24]
	Silver ion incorporation	Antibacterial, inhibit bacterial adhesion	[29,30,32,33,35]
	Silver and antibiotic hybrid coating	Enhanced antibacterial, anti-adhesion ability	[42,46]
	Antibacterial peptide coating	Antibacterial, inhibit biofilm formation	[48,76,77]
	Drug-loaded polymer modification	Antibacterial and hydrophobic	[78,79]
	Bacteriophage coating	Antibacterial	[26,80–83]
Functional coating on urinary devices	Polyether-based coating	Inhibit bacterial adhesion and improve the antibacterial properties	[86–88,90]
	Polyvinylpyrrolidone-iodine coating	Hydrophilicity, Inhibit bacterial adhesion	[93,94]
	Papain immobilized polyurethane	Antibiofilm ability	[97]
	Natural cyanobacterial coating	Inhibit bacterial adhesion	[98]
	Functional nanoparticles coating	Antibacterial and lubrication	[102,103,108]
Biodegradable polymers for urinary devices	Alginate biodegradable stent	Degradability	[109–112]
Metallic materials for urinary devices	Nickel alloy stent	Silhouette structure	[115,116,119]
	Cu-bearing stainless steel ureteral stents	Antibacterial	[121–123,130]
	Magnesium alloy degradable stent	Antibacterial and degradable	[110,111,133]
New oral composition drug	Crystallization inhibitors and urine acidifier	Decrease urine pH	[139]

encrustation test, the amount of calcium deposited on bare PU was approximately 51 mg and on papain immobilized was approximately 33 mg, and the amount of calcium plus magnesium deposited on bare PU was 50 mg, more than 40 mg on the modified polymer [97], which showed better anti-encrustation performance. However, few studies on the long-term benefit of anti-encrustation and its mechanical properties have been found. In vivo anti-encrustation properties should also be further investigated.

2.4. Natural cyanobacterial coating

A kind of marine cyanobacterium, named Natural Cyanobacterial Polymer-Based Coating (CyanoCoating), was used to develop a coating [98]. This coating has been proven to have good antiadhesion effects against *E. coli*, *S. aureus* and *P. aeruginosa*. Amazing biocompatibility also leads to potential applications in the future [99]. In this study, the authors grafted the CyanoCoating on the surface of a urinary catheter to evaluate its performance on anti UTI and encrustation in the urine environment. The results showed that CyanoCoating had great anti-adhesion ability against *E. coli* ($P < 0.05$), *S. aureus* ($P < 0.001$), and *Candida albicans* ($P < 0.001$). Moreover, it has great anti-bioform ability in *E. coli* ($P < 0.05$), *P. mirabilis* ($P < 0.01$), and Candida albicans ($P < 0.01$). Large crystals were found on the uncoated surface but not on the CyanoCoating based on the data from scanning electron microscopy (SEM). On the other hand, salt deposition was found on both surfaces. However, it is still unknown how long it is effective in anti-adhesion and anti-encrustation.

2.5. Functional nanoparticle coating

Fullerene-like MoS_2 (IF–MoS_2), a kind of inorganic layered nanoparticle compound, is effective in forming a seam-less closed-cage fullerene-like structure [100,101]. Every nanoparticle wrapped in a fully saturated van der Waals surface has a low affinity with the environment, making it easy for them to roll. When doped with rhenium to form electron rich Re-doped nanoparticles (Re: IF-MoS_2), they are self-assembled into a mosaic-like order, and the lubrication performance of this material is further increased [102]. The lubrication performance is effective in decreasing the development of encrustation on the catheter surface. A custom-built model of a catheterized urinary tract was used to conduct the in vitro encrustation process. The energy dispersive spectrometer (EDS) analysis also suggested that the Ca and P contents were 1.2% and 1.9% in the Re: IF-MoS_2-coated catheter, respectively, when compared with 10.1% and 8.6% in the uncoated specimen. This result was consistent with SEM (BSE and SE modes) imaging. The exact mechanism of Re: IF-MoS2-coated catheter encrustation suppression is not fully understood. Its self-assembling mosaic-like order might be the key to reducing deposits. Although some reports show that these nanoparticles have no toxic risk [103], their biocompatibility still needs further study in the future.

Chitosan (CS), produced by removing the acetate part of chitin through hydration in concentrated alkali, is a copolymer containing a β-(1,4)-2-acetamido-D-glucose and β-(1,4)-2-amino-D-glucose unit. Recent studies have shown that chitosan is known to have antibacterial potential thanks to its cationic polyelectrolyte nature to bind efficiently with negatively charged molecules and that chitosan-immobilized polyurethane materials have efficient antibacterial activity [104,105]. Chitosan nanoparticles (CSNPs), owing to their higher surface charge density, can more fully contact bacteria than chitosan [105–107]. CSNPs were immobilized on the PU ureter stent surface, and their ability to prevent bacterial adhesion was investigated. The results showed that in an in vitro antibacterial experiment, CSNP-coated stents showed good anti-*E. coli* and *P. mirabilis* properties by disrupting bacterial membranes through electrostatic interactions upon contact compared with the control group [108]. Because of its excellent killing ability against urease-producing bacteria, it can effectively inhibit bacterial adhesion and biofilm formation and has potential anti-encrustation properties, which need to be further investigated.

3. Biodegradable polymers for urinary devices

Polymer biodegradable materials have made remarkable progress in biomedicine. These biomaterials mainly include natural origin polymers, synthetic polymers and metals, which are characterized by biocompatibility, certain mechanical strength and biodegradability. Biodegradable ureteral stents are also attracting increasing attention [109]. The preparation methods of BUS mainly include winding, braiding, injection molding, and immersion technology [110]. They can provide sufficient mechanical support within a certain period of time to drain urine and then degrade into small particles excreted with the urine. They are mainly used in patients with short- and medium-term ureteral stent implantation, and those advantages are to avoid secondary operation to be removed and reduce medical costs. Continuous degradation and shedding of surface materials are also beneficial to resist the adhesion of bacteria and the formation of crystals. Long-term use is not suitable for patients, as the degradation time is not long enough. In addition, catheter degradation and broken fragments left in the urethra will produce strong lower urinary tract symptoms, making the patients extremely uncomfortable. This kind of degradable material is not suitable for use as a Foley catheter. Furthermore, the fragments in the degradation of the stents may lead to ureteral obstruction, hydronephrosis and nephritic damage [111]. Despite this, it still brings us an effective way to prevent encrustation.

Alginate is a biodegradable natural polymer. In 2002, Auge et al. made a ureteral stent with alginate, which was found to be degraded

completely after 7 days in pigs. Pathological examination showed that the material had no obvious toxicity to tissues in pigs [112]. In 2014, Barros et al. added gellan gum on the basis of alginate. Alginate, gellan gum, and their blends are gelated by physical cross-linking at low temperature, which obtains a stable structure by ion exchange, dehydration, solvent exchange and drying treatment (Fig. 6A) [113]. The stents made with different ratios increased the degradation time to 14–60 days in the degradation experiment in vitro. The encrustation test showed that no crystal formation was detected by SEM and EDS. Compared with other commercial stents, there was no significant change in cell viability between cytotoxicity and cell adhesion studies [114]. However, it fails to meet the mechanical strength in a certain period of time, and the degradation rate in vivo is faster than that in vitro, which is only approximately 10 days and makes it difficult to meet the needs of long-term placement of stents [110].

Biodegradable polymers ureteral stents have the advantage of not needing a second surgical removal due to the self-degradation property. At the same time, they are difficult to form encrustation because of the property. However, the potential stent obstruction caused by degradation substances and the rapid degradation cannot meet the needs of long-term indwelling catheters. The material surface peeling of biodegradable catheter/stent caused by degradation makes it difficult to form encrustation, and slow degradation is suitable for patients with long-term indwelling catheter/stent. So, how to long-term degradation or slow degradation is the problem need to be focused in the future.

4. Metallic materials for urinary devices

Two commercial metallic ureteral stents are currently available: one is the Silhouette stent produced by Applied Medical, Rancho Santa Margarita, and the other is the Resonance stent produced by Cook Medical, USA [115]. A silhouette stent is constructed with nitinol wire reinforcing the walls of the stent and covered with a polymer. Resonance stents are made up of nickel–cobalt–chromium–molybdenum alloy and have been used in the clinic for several decades [116]. They have higher strength than polymer stents and are suitable for many patients whose tumors oppress the ureter [117]. Many studies show that it can be approved for a maximum dwell time of at least 12 months [118]. However, after stents were removed, 22% of stents showed signs of encrustation [119]. Furthermore, its price in the United States is eight times higher than that of polymer stents. The total medical cost of replacing the stent also includes the cost of drugs and surgery. Despite the high price, long-term use can indeed reduce the financial burden of patients and the pain of surgery [120].

In recent years, researchers have found that copper (Cu) ions are a kind of antibacterial agent that has the long-term effect of inhibiting bacteria (including some drug-resistant bacteria) [121–123]. Other findings, such as that of metal nanoparticles (MNPs), including Cu or Cu oxide NPs, can kill bacteria by their ion mental interactions with nucleic acids, proteins and peptidoglycan of the cell wall [124–126]. A kind of hybrid system including copper ion modifying molybdenum disulfide (MoS_2) can release MoS_2 and copper ions to oxidize glutathione (GSH), which accelerates bacterial death and does little harm to the human body [127]. Other materials include Cu–TiO_2 nanofibers [128], Ag–Cu and Cu–Ag nanocomposites (NCs) [129]. In addition to their antibacterial properties, they are also effective in decreasing ureteral stent encrustation in vitro and in vivo. In 2017, researchers fabricated Cu-bearing stainless steel ureteral stents (Fig. 7A) and fewer crystal deposits on Cu-bearing stainless steel ureteral stents than uncoated stainless steel ureteral stents in an in vitro encrustation experiment (Fig. 7B and C). After the in vitro encrustation experiment, Cu-bearing stainless steel ureteral stents were implanted into the bladder of New Zealand rabbits for 20, 40 and 80 days, after which they killed the rabbits and removed the stents. They found that the material mentioned above can not only inhibit the adherence of microorganisms but also decrease encrustation formation in an in vivo model [130]. This anti-infection and encrustation mechanism is mainly because copper ions can inhibit the production of urease by bacteria, reduce the decomposition of urea into ammonia, and stabilize the urine pH [131]. Copper ions are known to have certain cytotoxic properties, and there is currently no evidence that the release of copper ions from this material will cause damage to urothelial cells. If it can be proven to be safe in terms of biocompatibility, this coating is ideal for long-term indwelling patients.

Metal has excellent mechanical properties, and magnesium alloys possess attractive biodegradability and biocompatibility properties and can be used as materials for biodegradable ureteral stents [110]. Some studies have shown that this magnesium alloy stent (Fig. 8A) has a bactericidal effect in the process of degradation, and the mechanism may be that magnesium nanoparticles penetrate the cell membrane of bacteria to kill it [114,132]. Jin et al. found that they had good antibacterial, biocompatibility and degradation times (4 weeks) on their magnesium and polymer mixed stents in vivo and in vitro (Fig. 8B) [111,133]. Their anti-encrustation ability was not tested in the above study. By their degradation performance and degradation mechanism, we can infer that this material has similar anti-encrustation performance as alginate, which needs to be further verified in future research.

The current metal material for urinary devices include alloy, nano-metal and biodegradable metal. Although alloy, nano-metal stent has obvious advantages in prevention of stent-related encrustation, but the alloy material is very expensive and nano metal stent lack of study of long-term biocompatibility. It is hard to form encrustation in biodegradable metal stent thanks to the biodegradable characteristics, however, there is no relevant research on anti-encrustation at present. Which we need to further investigate in the future.

5. New oral composition drug

A prolonged indwelling time of stents or catheters will result in urinary infection and encrustation of ureteral stents, which will lead to the use of extracorporeal lithotripsy, endourological or open surgery to resolve these conditions [134]. One reason for encrustation is the increase in pH, which will result in calcium and magnesium ions depositing on the biofilm [135]. Thus, if urine composition is altered by increasing urine acidification and the urine excretion of crystallization inhibitors, encrustation from the stent could be minimized. A new oral composition, which was first reported as a potential oral treatment to prevent ureteral stent-associated encrustation by changing the urine composition of the patients, contains both crystallization inhibitors (phytate) and a urine acidifier (L-methionine). Phytate, a sort of phytate salt that conforms to the inhibitory property of calcium salt deposits, was used to decrease the risk of encrustation formation [136]. L-Methionine is an essential amino acid that can directly reduce urine pH [137,138]. A randomized, double-blinded, and placebo-controlled trial containing a total of 105 patients was divided into two groups: the oral composition group and the placebo control group. The time of the clinical trial ranged from 3 to 8 weeks depending on the time lapses between the baseline visit and stent removal, and the average time was 37.54 $\pm$ 13.9 days. The results showed that the overall crust of the oral composition group was reduced by 8 times, and the pH reduction of the urine from baseline 1 to day 21 was also 0.47 lower than that of the placebo group [139]. The results revealed a significant decrease in stent encrustation in the intervention group. This confirmed that a higher urinary pH decrease was a protective factor against encrustation. If the effectiveness of crystal inhibition and low side effects in the course of long-term use can be verified, then the application of a new oral composition drug in the field of anti-catheter-associated encrustation is very promising.

6. Concluding remarks and future perspectives

Indwelling catheters can indeed solve many clinical problems, benefit many patients, slow down disease progression, reduce the incidence of complications, and reduce the average length of hospital stay. Due to the

limitations of the catheter design flaws and materials, there is no perfect solution, leading to catheter-related complications such as infection, encrustation, obstruction, pain, and hematuria. These complications cost the patients extra medical costs.

In recent years, promising technologies mainly include drug loading on urinary devices, functional coating on urinary devices, biodegradable polymers for urinary devices, metallic materials for urinary devices and new oral composition drug (Table 1). At present, a large amount of most popular research is the antibiotic release coating. One of the reasons is that antibiotics are the natural enemies of bacteria and can effectively kill bacteria. Moreover, close to interdisciplinary cooperation is not necessary in antibiotic coating research. Although the use of antibiotics is becoming increasingly standardized, drug resistance has always been a problem that has not been well solved. Drugs such as bacteriophages and enzymes are used as antibacterial materials; however, phage resistance and enzyme instability have not been well solved. Moreover, pharmacokinetics, coating release rate and other knowledge must be clearly understood when we develop the antibiotic release coating, which is difficult to accurately control without close multidisciplinary cooperation. Therefore, a non-release coating may be more suitable for patients with long-term indwelling catheters. At present, there are two main methods of non-release coating: 1, contact sterilization, in which the catheter surface is connected with antibacterial substances, such as antimicrobial peptides and other popular antimicrobial agents, with low drug resistance and broad-spectrum antibacterial activity. 2, the physical resistance to the adhesion of bacteria and biofilms and the anti-adhesion physical properties of the surface of polymers can resist the extracellular polysaccharides produced by bacteria so that bacteria cannot adhere or form biofilms on the surface of this material. It prevents the formation of crystals on the surface of the catheter, although it cannot kill bacteria, but it can prevent the occurrence of catheter stones. Of course, other methods, such as monitoring catheter obstruction and increasing water consumption, also play a role in preventing catheter stones.

It is difficult for clinicians to understand and apply relevant biomaterials, and experts who specialize in materials do not have a comprehensive understanding of clinical needs and problems. As the boundaries between biomaterials and medicine become increasingly blurred, the scope of their overlap becomes increasingly wider, which requires us to rethink the relationship between biomaterials and medicine. They must be closely related in some aspects. Therefore, multidisciplinary cooperation is necessary to make use of their respective advantages to combine different new technologies, new materials and new products. Although antibacterial coatings will still occupy most of the research on the development of anti-encrustation materials in the future, new materials, especially biomaterials with new characteristics, such as antimicrobial peptide coatings and brush antifouling coatings, will be further investigated in the future. Finally, it will be beneficial for patients who need long-term indwelling catheters.

Credit author statement

Qin Yao: Investigation, Writing-original draft, Chengshuai Wu, Xiaoyu Yu, Xu Chen: Investigation, Discussion, Guoqing Pan: Writing-review & editing, Binghai Chen: Conceptualization, Supervision, Writing-review & editing.

Declaration of competing interest

The authors declare that they have no known competing financial interests or personal relationships that could have appeared to influence the work reported in this paper.

Acknowledgments

This work was supported by the National Key Research and Development Program of China (2019YFA0112000), the National Natural Science Foundation of China (32222041 and 21875092), the Innovation and Entrepreneurship Program of Jiangsu Province, the “Six Talent Peaks” program of Jiangsu Province (2018-XCL-013), and the “Jiangsu Specially-Appointed Professor” Program, Natural Science Foundation of Jiangsu Province (BK20211123 and BK20220059), and Social Development Foundation of Zhenjiang (SH2021033).

Appendix A. Supplementary data

Supplementary data to this article can be found online at https://doi.org/10.1016/j.mtbio.2022.100413.

References

[1] M.L. Brodny, J. Urol. 60 (1948) 119–121.
[2] J.P. Herdman, Br. J. Surg. 37 (1949) 105.
[3] C.R. Riedl, E. Plas, W.A. Hubner, H. Zimmerl, W. Ulrich, H. Pfluger, Eur. Urol. 36 (1999) 53–59.
[4] R.C. Feneley, I.B. Hopley, P.N. Wells, J. Med. Eng. Technol. 39 (2015) 459–470.
[5] S. Saint, C.E. Chenoweth, Infect. Dis. Clin. 17 (2003) 411–432.
[6] W. Yin, Y. Wang, L. Liu, J. He, Int. J. Mol. Sci. 20 (2019).
[7] C.W. Hall, T.F. Mah, FEMS Microbiol. Rev. 41 (2017) 276–301.
[8] M. Ramstedt, I.A.C. Ribeiro, H. Bujdakova, F.J.M. Mergulhão, L. Jordao, P. Thomsen, M. Alm, M. Burmølle, T. Vladkova, F. Can, M. Reches, M. Riool, A. Barros, R.L. Reis, E. Meaurio, J. Kikhney, A. Moter, S.A.J. Zaat, J. Sjollema, Macromol. Biosci. 19 (2019), e1800384.
[9] P. Singha, J. Locklin, H. Handa, Acta Biomater. 50 (2017) 20–40.
[10] A. Torzewska, A. Rozalski, Microbiol. Res. 169 (2014) 579–584.
[11] M.G. Menegueti, M.A. Ciol, F. Bellissimo-Rodrigues, M. Auxiliadora-Martins, G.G. Gaspar, S. Canini, A. Basile-Filho, A.M. Laus, Medicine (Baltim.) 98 (2019), e14417.
[12] C.E. Chenoweth, Infect. Dis. Clin. 35 (2021) 857–870.
[13] M.M. Schiessler, L.M. Darwin, A.R. Phipps, L.R. Hegemann, B.S. Heybrock, A.J. Macfadyen, Pediatr Qual Saf 4 (2019) e183.
[14] J.R. Johnson, B. Johnston, M.A. Kuskowski, Antimicrob. Agents Chemother. 56 (2012) 4969–4972.
[15] X. Zhao, K. Drlica, Clin. Infect. Dis. 33 (Suppl 3) (2001) S147–S156.
[16] A.D. Russell, Lancet Infect. Dis. 3 (2003) 794–803.
[17] T. Xu, M. Deshmukh, V.M. Barnes, H.M. Trivedi, D. Cummins, Comp. Cont. Educ. Dent. 25 (2004) 46–53.
[18] M. Mustafa, B. Wondimu, T. Yucel-Lindberg, A.T. Kats-Hallstrom, A.S. Jonsson, T. Modeer, J. Clin. Periodontol. 32 (2005) 6–11.
[19] P.A. Cadieux, B.H. Chew, L. Nott, S. Seney, C.N. Elwood, G.R. Wignall, L.W. Goneau, J.D. Denstedt, J. Endourol. 23 (2009) 1187–1194.
[20] A.J. McBain, R.G. Ledder, P. Sreenivasan, P. Gilbert, J. Antimicrob. Chemother. 53 (2004) 772–777.
[21] A.J. McBain, R.G. Bartolo, C.E. Catrenich, D. Charbonneau, R.G. Ledder, B.B. Price, P. Gilbert, Appl. Environ. Microbiol. 69 (2003) 5433–5442.
[22] H. Hao, J. Shao, Y. Deng, S. He, F. Luo, Y. Wu, J. Li, H. Tan, J. Li, Q. Fu, Biomater. Sci. 4 (2016) 1682–1690.
[23] Y. Tian, Z. Jian, J. Wang, W. He, Q. Liu, K. Wang, H. Li, H. Tan, Int. Urol. Nephrol. 49 (2017) 563–571.
[24] K. Belfield, X. Chen, E.F. Smith, W. Ashraf, R. Bayston, Acta Biomater. 90 (2019) 157–168.
[25] K. Belfield, H. Betts, R. Parkinson, R. Bayston, Neurourol. Urodyn. 38 (2019) 338–345.
[26] A. Majeed, F. Sagar, A. Latif, H. Hassan, A. Iftikhar, R.O. Darouiche, M.A. Mohajer, Expet Rev. Med. Dev. 16 (2019) 809–820.
[27] S.D. Morgan, D. Rigby, D.J. Stickler, Urol. Res. 37 (2009) 89–93.
[28] R. Wang, K.G. Neoh, E.T. Kang, P.A. Tambyah, E. Chiong, J. Biomed. Mater. Res. B Appl. Biomater. 103 (2015) 519–528.
[29] M. Chen, P.O. Zamora, P. Som, L.A. Pena, S. Osaki, J. Biomater. Sci. Polym. Ed. 14 (2003) 917–935.
[30] Q. Zhao, Y. Liu, C. Wang, Appl. Surf. Sci. 252 (2005) 1620–1627.
[31] L. Wang, S. Zhang, R. Keatch, G. Corner, G. Nabi, S. Murdoch, F. Davidson, Q. Zhao, J. Hosp. Infect. 103 (2019) 55–63.
[32] H. Lee, S.M. Dellatore, W.M. Miller, P.B. Messersmith, Science 318 (2007) 426–430.
[33] G. Cheng, Z. Zhang, S. Chen, J.D. Bryers, S. Jiang, Biomaterials 28 (2007) 4192–4199.
[34] K.D. Mandakhalikar, R. Wang, J.N. Rahmat, E. Chiong, K.G. Neoh, P.A. Tambyah, BMC Infect. Dis. 18 (2018) 370.

[35] H. Heidari Zare, V. Juhart, A. Vass, G. Franz, D. Jocham, Biointerphases 12 (2017), 011001.
[36] K.P. Srinivasakumar, R. Mala, A.A. Aglin, S. Kiruthika, C. Vazagapriya.
[37] R. Mala, A. Annie Aglin, A.S. Ruby Celsia, S. Geerthika, N. Kiruthika, C. VazagaPriya, K. Srinivasa Kumar, IET Nanobiotechnol. 11 (2017) 612–620.
[38] P.C. Appelbaum, P.A. Hunter, Int. J. Antimicrob. Agents 16 (2000) 5–15.
[39] T.M. Hooton, Infect. Dis. Clin. 17 (2003) 303–332.
[40] C.M. Oliphant, G.M. Green, Am. Fam. Physician 65 (2002) 455–464.
[41] K.S. Siddiqi, A. Husen, R.A.K. Rao, J. Nanobiotechnol. 16 (2018) 14.
[42] E. Dayyoub, M. Frant, S.R. Pinnapireddy, K. Liefeith, U. Bakowsky, Int. J. Pharm. 531 (2017) 205–214.
[43] M. Frant, E. Dayyoub, U. Bakowsky, K. Liefeith, Int. J. Pharm. 546 (2018) 86–96.
[44] S. Ullah, M. Hashmi, D. Kharaghani, M.Q. Khan, Y. Saito, T. Yamamoto, J. Lee, I.S. Kim, Int. J. Nanomed. 14 (2019) 2693–2703.
[45] N. Duran, M. Duran, M.B. de Jesus, A.B. Seabra, W.J. Favaro, G. Nakazato, Nanomedicine 12 (2016) 789–799.
[46] A.R. El-Nahas, M. Lachine, E. Elsawy, A. Mosbah, H. El-Kappany, Scand J Urol 52 (2018) 76–80.
[47] J.M. Ageitos, A. Sánchez-Pérez, P. Calo-Mata, T.G. Villa, Biochem. Pharmacol. 133 (2017) 117–138.
[48] C. Monteiro, F. Costa, A.M. Pirttila, M.V. Tejesvi, M.C.L. Martins, Sci. Rep. 9 (2019), 10753.
[49] M. Zasloff, Nature 415 (2002) 389–395.
[50] S.A. Baltzer, M.H. Brown, J. Mol. Microbiol. Biotechnol. 20 (2011) 228–235.
[51] J. Fernebro, Drug Resist. Updates 14 (2011) 125–139.
[52] G. Laverty, S.P. Gorman, B.F. Gilmore, Int. J. Mol. Sci. 12 (2011) 6566–6596.
[53] M.D. Seo, H.S. Won, J.H. Kim, T. Mishig-Ochir, B.J. Lee, Molecules 17 (2012) 12276–12286.
[54] K.A. Brogden, Nat. Rev. Microbiol. 3 (2005) 238–250.
[55] A.C. Rios, C.G. Moutinho, F.C. Pinto, F.S. Del Fiol, A. Jozala, M.V. Chaud, M.M. Vila, J.A. Teixeira, V.M. Balcao, Microbiol. Res. 191 (2016) 51–80.
[56] J.M. Sierra, E. Fusté, F. Rabanal, T. Vinuesa, M. Viñas, Expet Opin. Biol. Ther. 17 (2017) 663–676.
[57] M.R. Yeaman, N.Y. Yount, Pharmacol. Rev. 55 (2003) 27–55.
[58] Akhilesh, Pinto, Sandra, Evangelista, B. Marta Helena, Kallip, Silvar, Ferreira, G.S. Mario.
[59] F. Costa, S.R. Maia, P. Gomes, M. Martins, Biomaterials 52 (2015) 531–538.
[60] K. Yu, J. Lo, M. Yan, X. Yang, D.E. Brooks, R. Hancock, D. Lange, J.N. Kizhakkedathu, Biomaterials 116 (2017) 69–81.
[61] M.D.P. Willcox, E.B.H. Hume, Y. Aliwarga, N. Kumar, N. Cole, J. Appl. Microbiol. 105 (2008).
[62] H. Lee, B.P. Lee, P.B. Messersmith, Nature 448 (2007) 338–341.
[63] G.P. Maier, M.V. Rapp, J.H. Waite, J.N. Israelachvili, A. Butler, Science 349 (2015) 628–632.
[64] J.H. Ryu, P.B. Messersmith, H. Lee, ACS Appl. Mater. Interfaces 10 (2018) 7523–7540.
[65] J. Liebscher, R. Mrowczynski, H.A. Scheidt, C. Filip, N.D. Hadade, R. Turcu, A. Bende, S. Beck, Langmuir 29 (2013) 10539–10548.
[66] M. d'Ischia, A. Napolitano, V. Ball, C.T. Chen, M.J. Buehler, Acc. Chem. Res. 47 (2014) 3541–3550.
[67] J. Yang, M.A. Cohen Stuart, M. Kamperman, Chem. Soc. Rev. 43 (2014) 8271–8298.
[68] J. Yu, Y. Kan, M. Rapp, E. Danner, W. Wei, S. Das, D.R. Miller, Y. Chen, J.H. Waite, J.N. Israelachvili, Proc. Natl. Acad. Sci. U. S. A. 110 (2013) 15680–15685.
[69] S.A. Mian, L.M. Yang, L.C. Saha, E. Ahmed, M. Ajmal, E. Ganz, Langmuir 30 (2014) 6906–6914.
[70] D. Song, L. Chen, T. Li, Z.R. Xu, Colloids and Interface Science Communications 40 (2021), 100340.
[71] X. Chen, Y. Gao, Y. Wang, G. Pan, Smart Materials in Medicine 2 (2021) 26–37.
[72] Y. Xiao, W. Wang, X. Tian, X. Tan, Z. Yang, Research 2020 (2020) 1–12.
[73] J. Bai, H. Wang, H. Chen, G. Ge, D. Geng, Biomaterials 255 (2020), 120197.
[74] Y. Liu, K. Ai, L. Lu, Chem. Rev. 114 (2014) 5057–5115.
[75] T.K. Das, S. Ganguly, S. Ghosh, S. Remanan, N.C. Das, Colloids and Interface Science Communications 33 (2019), 100218.
[76] Q. Yao, B. Chen, J. Bai, W. He, X. Chen, D. Geng, G. Pan, J. Mater. Chem. B (2022), 2584-2596.
[77] K. Yu, J.C. Lo, M. Yan, X. Yang, D.E. Brooks, R.E. Hancock, D. Lange, J.N. Kizhakkedathu, Biomaterials 116 (2017) 69–81.
[78] S. Movassaghian, O.M. Merkel, V.P. Torchilin, Wiley Interdiscip Rev Nanomed Nanobiotechnol 7 (2015) 691–707.
[79] C.P. McCoy, N.J. Irwin, L. Donnelly, D.S. Jones, J.G. Hardy, L. Carson, Int. J. Pharm. 535 (2018) 420–427.
[80] S.M. Lehman, R.M. Donlan, Antimicrob. Agents Chemother. 59 (2015) 1127–1137.
[81] K.S. Liao, S.M. Lehman, D.J. Tweardy, R.M. Donlan, B.W. Trautner, J. Appl. Microbiol. 113 (2012) 1530–1539.
[82] W. Fu, T. Forster, O. Mayer, J.J. Curtin, S.M. Lehman, R.M. Donlan, Antimicrob. Agents Chemother. 54 (2010) 397–404.
[83] J.J. Curtin, R.M. Donlan, Antimicrob. Agents Chemother. 50 (2006) 1268–1275.
[84] S. Milo, H. Hathaway, J. Nzakizwanayo, D.R. Alves, P.P. Esteban, B.V. Jones, A.T.A. Jenkins, J. Mater. Chem. B 5 (2017) 5403–5411.
[85] J. Nzakizwanayo, A. Hanin, D.R. Alves, B. McCutcheon, C. Dedi, J. Salvage, K. Knox, B. Stewart, A. Metcalfe, J. Clark, B.F. Gilmore, C.G. Gahan, A.T. Jenkins, B.V. Jones, Antimicrob. Agents Chemother. 60 (2015) 1530–1536.
[86] X.H. Hu, G.J. Zhang, H.P. Tan, D. Li, X.Y. Chen, Y.S. Zhang, Mater. Technol. 29 (2013) 144–151.
[87] M. Alinejad, C. Henry, S. Nikafshar, A. Gondaliya, S. Bagheri, N. Chen, S.K. Singh, D.B. Hodge, M. Nejad, Polymers (2019) 11.
[88] Z.A. Uwais, M.A. Hussein, M.A. Samad, N. Al-Aqeeli, Arabian J. Sci. Eng. 42 (2017) 4493–4512.
[89] C.M. Cottone, S. Lu, Y.X. Wu, K. Guan, R. Yoon, L. Limfueco, T. Hoang, W. Ciridon, B.D. Ratner, K.R. Johnson, R.M. Patel, J. Landman, R.V. Clayman, J. Endourol. 34 (2020) 868–873.
[90] J. Lin, S. Qiu, K. Lewis, A.M. Klibanov, Biotechnol. Prog. 18 (2002) 1082–1086.
[91] M. Gultekinoglu, Y. Tunc Sarisozen, C. Erdogdu, M. Sagiroglu, E.A. Aksoy, Y.J. Oh, P. Hinterdorfer, K. Ulubayram, Acta Biomater. 21 (2015) 44–54.
[92] M. Gultekinoglu, B. Kurum, S. Karahan, D. Kart, M. Sagiroglu, N. Ertas, A. Haluk Ozen, K. Ulubayram, Mater Sci Eng C Mater Biol Appl 71 (2017) 1166–1174.
[93] S.A. Holmes, C. Cheng, H.N. Whitfield, Br. J. Urol. 69 (1992) 651–655.
[94] A.P. Khandwekar, M. Doble, J. Mater. Sci. Mater. Med. 22 (2011) 1231–1246.
[95] J. Drenth, J.N. Jansonius, R. Koekoek, H.M. Swen, B.G. Wolthers, Nature 218 (1968) 929–932.
[96] B. Tpa, D. Msc, B. Cv, E. Bm, G. Mrkf, I. Flc, Int. J. Biol. Macromol. 188 (2021) 94–113.
[97] C. Maria Manohar, M. Doble, J. Biomed. Mater. Res. B Appl. Biomater. 104 (2016) 723–731.
[98] R. Mota, R. Guimaraes, Z. Buttel, F. Rossi, G. Colica, C.J. Silva, C. Santos, L. Gales, A. Zille, R. De Philippis, S.B. Pereira, P. Tamagnini, Carbohydr. Polym. 92 (2013) 1408–1415.
[99] B. Costa, R. Mota, P. Parreira, P. Tamagnini, F. Costa, Mar. Drugs 17 (2019).
[100] R. Ron, D. Zbaida, I.Z. Kafka, R. Rosentsveig, I. Leibovitch, R. Tenne, Nanoscale 6 (2014) 5251–5259.
[101] T.M. Hamill, B.F. Gilmore, D.S. Jones, S.P. Gorman, Expet Rev. Med. Dev. 4 (2007) 215–225.
[102] L. Yadgarov, R. Rosentsveig, G. Leitus, A. Albu-Yaron, A. Moshkovich, V. Perfilyev, R. Vasic, A.I. Frenkel, A.N. Enyashin, G. Seifert, L. Rapoport, R. Tenne, Angew Chem. Int. Ed. Engl. 51 (2012) 1148–1151.
[103] H. Wu, R. Yang, B. Song, Q. Han, J. Li, Y. Zhang, Y. Fang, R. Tenne, C. Wang, ACS Nano 5 (2011) 1276–1281.
[104] K. Kakaei, M. Esrafili, A. Ehsani, Interface Science and Technology 27 (2019) 67–108.
[105] E.I. Rabea, E.T. Badawy, C.V. Stevens, G. Smagghe, W. Steurbaut, Biomacromolecules 4 (2003) 1457.
[106] M. Jia, Y. Li, X. Yang, Y. Huang, H. Wu, Y. Huang, J. Lin, Y. Li, Z. Hou, Q. Zhang, ACS Appl. Mater. Interfaces 6 (2014), 11413.
[107] S. Sanyakamdhorn, D. Agudelo, H.A. Tajmir-Riahi, Biomacromolecules 14 (2013) 557–563.
[108] G.V. Kumar, C.H. Su, P. Velusamy, Biofouling 32 (2016) 861–870.
[109] B.H. Chew, D. Lange, Curr. Opin. Urol. 26 (2016) 277–282.
[110] L. Wang, G. Yang, H. Xie, F. Chen, J. Biomater. Sci. Polym. Ed. 29 (2018) 1657–1666.
[111] L. Jin, L. Yao, F. Yuan, G. Dai, B. Xue, J. Biomed. Mater. Res. B Appl. Biomater. (2020), 665-672.
[112] B.K. Auge, R.F. Ferraro, A.R. Madenjian, G.M. Preminger, J. Urol. 168 (2002) 808–812.
[113] A.R.C. Duarte, V.E. Santo, A. Alves, S.S. Silva, J. Moreira-Silva, T.H. Silva, A.P. Marques, R.A. Sousa, M.E. Gomes, J.F. Mano, R.L. Reis, J. Supercrit. Fluids 79 (2013) 177–185.
[114] A.A. Barros, A. Rita, C. Duarte, R.A. Pires, B. Sampaio-Marques, P. Ludovico, E. Lima, J.F. Mano, R.L. Reis, J. Biomed. Mater. Res. B Appl. Biomater. 103 (2015) 608–617.
[115] C. Forbes, K.B. Scotland, D. Lange, B.H. Chew, Urol. Clin. 46 (2019) 245–255.
[116] S.D. Blaschko, L.A. Deane, A. Krebs, C.S. Abdelshehid, F. Khan, J. Borin, A. Nguyen, E.M. McDougall, R.V. Clayman, J. Endourol. 21 (2007) 780–783.
[117] M.S. Christman, O. L'Esperance, C.H. Choe, S.P. Stroup, B.K. Auge, J. Urol. 181 (2009) 392–396.
[118] M.S. Christman, J.O. L'Esperance, C.H. Choe, S.P. Stroup, B.K. Auge, BJU Int. 105 (2010) 866–869, discussion 868-869.
[119] Liatsikos Evangelos, Kallidonis Panagiotis, Kyriazis Iason, Constantinos, Eur. Urol. (2010), 480-487.
[120] A.J. Polcari, C.M. Hugen, H.L. Lopez-Huertas, T.M. Turk, Expert Rev. Pharmacoecon. Outcomes Res. 10 (2010) 11–15.
[121] C.D. Tran, J. Makuvaza, E. Munson, B. Bennett, ACS Appl. Mater. Interfaces 9 (2017) 42503–42515.
[122] S. Chen, J. Popovich, W. Zhang, C. Ganser, S.E. Haydel, D.K. Seo, RSC Adv. 8 (2018) 37949–37957.
[123] Q. Xu, M. Chang, Y. Zhang, E. Wang, M. Xing, L. Gao, Z. Huan, F. Guo, J. Chang, ACS Appl. Mater. Interfaces 12 (2020) 31255–31269.
[124] K. Gold, B. Slay, M. Knackstedt, A.K. Gaharwar, Advanced Therapeutics 1 (2018).
[125] M. Alavi, N. Karimi, Int. J. Biol. Macromol. 128 (2019) 893–901.
[126] P.K. Baruah, I. Chakrabartty, D.S. Mahanta, L. Rangan, A.K. Sharma, A. Khare, Rev. Sci. Instrum. 91 (2020), 034105.

[127] C. Wang, J. Li, X. Liu, Z. Cui, D.F. Chen, Z. Li, Y. Liang, S. Zhu, S. Wu, Biomater. Sci. (2020), 4216-4224.
[128] X. Zheng, Z.P. Shen, C. Cheng, L. Shi, R. Cheng, D.H. Yuan, Environ. Pollut. 237 (2018) 452–459.
[129] M. Alavi, N. Karimi, Artif. Cell Nanomed. Biotechnol. 46 (2018) S399–S413.
[130] J. Zhao, Z. Cao, H. Lin, H. Yang, J. Li, X. Li, B. Zhang, K. Yang, J. Mater. Sci. Mater. Med. 30 (2019) 83.
[131] J. Zhao, L. Ren, B. Zhang, Z. Cao, K. Yang, J. Mater. Sci. Technol. 33 (2017) 1604–1609.
[132] J.Y. Lock, E. Wyatt, S. Upadhyayula, A. Whall, V. Nunez, V.I. Vullev, H. Liu, J. Biomed. Mater. Res. 102 (2014) 781–792.
[133] L. Jin, L. Yao, Y. Zhou, G. Dai, W. Zhang, B. Xue, J. Biomater. Appl. 33 (2018) 466–473.
[134] A.M. Acosta-Miranda, J. Milner, T. Turk, J. Endourol. 23 (2009) 409–415.
[135] A. Mosayyebi, C. Manes, D. Carugo, B.K. Somani, Curr. Urol. Rep. 19 (2018) 35.
[136] F. Grases, B. Isern, P. Sanchis, J. Perello, J.J. Torres, A. Costa-Bauza, Front. Biosci. : J. Vis. Literacy 12 (2007) 2580–2587.
[137] R. Siener, F. Struwe, A. Hesse, Urology 98 (2016) 39–43.
[138] M. Passaro, G. Mainini, F. Ambrosio, R. Sgambato, G. Balbi, J. Alternative Compl. Med. 23 (2017) 471–478.
[139] C. Torrecilla, J. Fernandez-Concha, J.R. Cansino, J.A. Mainez, J.H. Amon, S. Costas, O. Angerri, E. Emiliani, M.A. Arrabal Martin, M.A. Arrabal Polo, A. Garcia, M.C. Reina, J.F. Sanchez, A. Budia, D. Perez-Fentes, F. Grases, A. Costa-Bauza, J. Cune, BMC Urol. 20 (2020) 65.